

UCD-96-31
 LBNL-39474
 October, 1996

Determining the existence and nature of the quark-gluon plasma by Upsilon suppression at the LHC

J.F. GUNION[†]

*Davis Institute for High Energy Physics, Physics Department,
 University of California, Davis, California 95616 USA*

R. VOGT^{*}

*Nuclear Science Division,
 Lawrence Berkeley National Laboratory, Berkeley, California 94720
 and
 Physics Department,
 University of California, Davis, California 95616 USA*

Abstract

Minijet production in $\sqrt{s} = 5.5$ TeV Pb+Pb collisions at the LHC is expected to produce a gluon-dominated plasma with large initial temperatures and energy densities. We discuss the implications of the high initial temperatures on the screening mass and on the relative suppression of members of the Υ family. We demonstrate that p_T -dependence of the Υ'/Υ ratio is only expected if a quark-gluon plasma with significant energy density is present, and that the precise dependence of this ratio will strongly constrain the QGP models. We also propose that the p_T spectra of the Υ resonances themselves will provide valuable information by comparing these spectra to that of the Z boson, which should not be influenced by plasma production.

[†]Supported by the Department of Energy under Contract No. DE-FG03-91ER40674 and by the Davis Institute for High Energy Physics.

^{*}This work was supported in part by the Director, Office of Energy Research, Division of Nuclear Physics of the Office of High Energy and Nuclear Physics of the U. S. Department of Energy under Contract No. DE-AC03-76SF0098.

1 Introduction

Finite temperature simulations of lattice gauge theory suggest a phase transition at high energy density and temperature to a new phase of QCD matter — the quark-gluon plasma (QGP). In many models, the temperatures and energy densities reached in central nucleus-nucleus collisions at the Brookhaven Relativistic Heavy Ion Collider (RHIC) and the Large Hadron Collider (LHC) at CERN are predicted to be sufficient for QGP formation. Demonstrating that such a QGP has formed and understanding its nature will be a very important component of the experimental programs at both machines. In this paper, we focus on using measurements of the p_T spectra of the Upsilon resonance family to accomplish these tasks, emphasizing the possible advantages of the higher LHC energy as compared to RHIC energy.

The details of the QCD phase transition to the QGP, as obtained in finite temperature simulations of lattice gauge theory, are strongly dependent on the number of quark flavors, n_f , and the number of colors, N . The critical temperature, T_c , and the order of the phase transition are particularly sensitive to the values of n_f and N used in the simulations [1]. In a pure $SU(N)$ gauge theory, $n_f = 0$, the phase transition is second order, *i.e.* continuous, for $SU(2)$ and first order for $SU(3)$. For the $SU(N)$ theory, the critical temperature, T_c , is 260 MeV. When dynamical light quarks are included in the lattice simulation, the critical temperature is substantially lower and the order of the phase transition can be altered: for $n_f = 2$, $T_c \approx 150$ MeV and the phase transition appears to be continuous; for simulations with more light flavors, $n_f \geq 3$, T_c is unaltered but the transition again becomes first order. This latter conclusion depends on the relative quark masses [2]. The critical energy density at T_c is only weakly dependent on the color and flavor degrees of freedom; $\epsilon_c \approx 1 - 2 \text{ GeV}/\text{fm}^3$ is obtained both with and without quark degrees of freedom for $N = 2$ or 3. For a QGP to be formed in an ultrarelativistic heavy-ion collision, the initial temperature, T_0 , and energy density, $\epsilon(t_0)$, of the quark-gluon system created by the collision must be larger than T_c and ϵ_c .

Part of the LHC experimental program will be devoted to heavy ion collisions such as Pb+Pb at $\sqrt{s} = 5.5$ TeV. At this high energy, the highest available for heavy-ion collisions, perturbative QCD processes will be the dominant factor in determining the initial state of the post-collision quark/gluon system. In particular, at early times, $t_0 \sim 1/p_T \leq 1/p_0$, semihard production of minijets¹ could be dominant in establishing the initial conditions for further evolution of the system [5]. The appropriate value of p_0 is uncertain but should be of order $p_0 \sim 2 \text{ GeV}$, in which case $t_0 \sim 0.1 \text{ fm}$. The crucial

¹Minijets are jets with $p_T \geq p_0 \sim 1 - 3 \text{ GeV}$ [3], usually not observable as individual jets below $p_T \sim 5 \text{ GeV}$ [4].

quantity in determining whether a quark-gluon plasma forms is the initial energy density, given by

$$\epsilon(t_0) = \frac{\overline{E}_T p_0}{\pi R^2}, \text{ with } \overline{E}_T = T_{AA}(\mathbf{0}) \sigma_{\text{jet}} \langle E_T \rangle. \quad (1)$$

Here, R is of order the nuclear radius, R_A , $T_{AA}(\mathbf{0})$ is the nuclear overlap for a central collision² and $\sigma_{\text{jet}} \langle E_T \rangle$ is the first p_T moment of the minijet production cross section in the central unity of rapidity in pp collisions (if we neglect nuclear shadowing) using the assumed value of p_0 . The initial temperature T_0 is proportional to $[\epsilon(t_0)]^{1/4}$. For given p_0 , $\sigma_{\text{jet}} \langle E_T \rangle$ is computable from QCD once the parton distribution functions (PDF's) for the colliding protons and the types of jets participating in the plasma are both specified. If we take $p_0 = 2 \text{ GeV}$, employ MRS D-' [6] parton densities and include only gluon jets (*i.e.* assume a pure gluon plasma) with rapidity $|y| \leq 0.5$, then the semihard production of minijets leads to a large initial energy density, $\epsilon(t_0) = 1170 \text{ GeV/fm}^3$, and initial temperature, $T_0 = 1.14 \text{ GeV}$, in central Pb+Pb collisions at $\sqrt{s} = 5.5 \text{ TeV}$, to be compared to $\epsilon(t_0) = 27 \text{ GeV/fm}^3$ and $T_0 = 0.46 \text{ GeV}$ at the lower RHIC energy. See [7, 8] for details.

The sensitivity of the critical parameters to the choice of PDF set is illustrated in Table 1, following [7, 8]. MRS D-' provides the most optimistic initial temperature, with the MRS H distributions [9] (designed to fit early HERA data) not far behind. The Duke-Owens-I (DO1) [10], and MRS D0' [6] distributions that grow more slowly as x decreases yield smaller initial energy density. More recent HERA data continues to favor distributions (such as the MRS A parameterization [11]) that at small x are similar to the H parameterization, *i.e.* that do not grow quite so rapidly at small- x as the D-' distributions but are certainly much more singular than either DO1 or D0'. All the numbers quoted in the table will become smaller when reductions in parton density due to shadowing in the nucleus are incorporated.

The sensitivity of the results to p_0 depends upon the PDFs. Increasing p_0 from 2 to 4 GeV decreases $\sigma_{\text{jet}} \langle E_T \rangle$ by factors of 5, 3, 2, and 1.5 for D-' [6], H [9], D0' [6], and DO1 [10] distributions, respectively, at $\sqrt{s} = 5.5 \text{ TeV}$. However, $\epsilon(t_0)$, eq. (1), also proportional to p_0 , changes by a factor of two or less, even increasing in the DO1 case. The sensitivity of $\epsilon(t_0)$ to p_0 at RHIC is much greater, declining by as much as a factor of 5 between $p_0 = 2 \text{ GeV}$ and $p_0 = 4 \text{ GeV}$. Inclusion of quark as well as gluon jets would increase $\epsilon(t_0)$ by roughly 30% at $\sqrt{s} = 5.5 \text{ TeV}$, but if the plasma is a quark-gluon plasma with 2 to 3 active flavors, the equation of state changes so that T_0 actually declines.

²The nuclear overlap function for a collision of projectile A with target B is $T_{AB}(\mathbf{b}) = \int d^2\mathbf{s} dz dz' \rho_A(\mathbf{s}, z) \rho_B(\mathbf{b} - \mathbf{s}, z')$ where the impact parameter \mathbf{b} is zero in the most central collisions.

PDF	#jets	# gluon jets	\overline{E}_T (GeV)	T_0 (GeV)	$dN_{\text{ch}}^{\text{gluons only}}/dy$
DO1	776	640	3200	0.74	914
D0'	1510	1250	5440	0.81	1350
H	3250	2710	10300	0.96	2130
D-'	5980	5220	17600	1.14	3360

Table 1: Dependence of initial temperature and particle density on distribution function choice at $\sqrt{s} = 5.5$ TeV. The results are taken from Ref. [8]. We employ $T_{\text{PbPb}}(\mathbf{0}) = 32 \text{ mb}^{-1}$. The distributions employed are Duke-Owens I, DO1 [10], the MRS D0' and D- ' from [6], and the MRS H distributions from [9].

Regardless of the parameters employed, it is apparent that minijet production yields substantially larger initial temperatures than previously predicted (for example, in Ref. [12]) and thus enhances the possibility of QGP production in thermal equilibrium. Only the extent of this enhancement is uncertain. For large enough p_0 and/or extensive nuclear shadowing, the energy density and temperature might be reduced sufficiently that the plasma would not be fully equilibrated, although a QGP might still be formed. In any case, it is important to examine the proposed signatures of plasma formation for the increased initial energy density and temperature obtained after including the effects of minijet production.

One of the proposed signatures of the QCD phase transition is the suppression of quarkonium production, particularly of the J/ψ [13, 14]. In fact, J/ψ and ψ' suppression have been observed in nucleus-nucleus collisions at the CERN SPS with $\sqrt{s} = 19.4$ GeV [15, 16]. In a QGP, the suppression occurs due to the shielding of the $c\bar{c}$ binding potential by color screening, leading to the breakup of the resonance. The $c\bar{c}$ (J/ψ , ψ' , \dots) and $b\bar{b}$ (Υ , Υ' , \dots) resonances have smaller radii than light-quark hadrons and therefore higher temperatures are needed to disassociate these quarkonium states. At current energies, the situation for the J/ψ is rather ambiguous because the bound state can also break up through interactions with nucleons and comoving hadrons—QGP production is not a unique explanation of J/ψ suppression [17, 18, 19, 20]. At LHC energies there will continue to be ambiguity in this regard, and, in addition, J/ψ and ψ' detection efficiencies may not be large [21].

In contrast, the Υ resonances are sufficiently tightly bound that it is more difficult to break them up as a consequence of ordinary multiple interactions. In addition, they can be detected in the $\mu^+\mu^-$ decay mode with relatively high efficiency at the LHC (*e.g.* 33% vs. 6% for J/ψ in the CMS detector

[21]). Further, this detection efficiency derives entirely from the central region ($|\eta| < 2.4$ in the CMS detector [21]), where the predictions for the relative suppression of the members of the Υ family in the presence of a gluon plasma can be most reliably tested (given that the baryon density is predicted to be low and should not play a significant role). However, it was previously assumed that the Υ would not be suppressed by QGP production [14, 22], since the Υ is much smaller than the $c\bar{c}$ and other $b\bar{b}$ resonances (such as the Υ' and χ_b states), implying that a much higher temperature than expected from earlier estimates of T_0 is needed to dissociate the Υ [14]. In view of the high initial temperature of a gluon plasma, $T_0 \approx 1$ GeV, when minijets are included, a reexamination of this assumption is in order. If Υ suppression by a minijet plasma is predicted, the Υ may provide a cleaner plasma signature than the J/ψ because of its weaker interactions with matter. In high energy heavy-ion collisions, the Υ rate should be large enough to test the predictions given here and help clarify the initial state of the system.

The paper is organized as follows. In the next section, we review the model of quarkonium suppression in a QGP and introduce two different scenarios for quarkonium breakup at finite temperature. Section 3 presents the quarkonium production model we adopt and includes a discussion of the expected Υ production rate. We then provide a detailed examination of Υ family suppression in a minijet plasma as a function of p_T and discuss the sensitivity of the results to the initial conditions. In section 5, we elucidate the steps necessary to extract information on the state of the system. We particularly focus on the Υ'/Υ ratio and discuss the effect of cascade decays from higher states on the signal. We also propose using the Z boson as a reference process against which Υ suppression can be tested. In summary, we show that the Υ family may provide an extremely powerful tool for diagnosing the existence and nature of the quark-gluon plasma.

2 Quarkonia in a quark-gluon plasma

We follow the arguments of Ref. [14] to discuss the finite temperature properties of quarkonium. The interquark potential for nonrelativistically bound quarkonium at zero temperature is

$$V(r, 0) = \sigma r - \frac{\alpha}{r}, \quad (2)$$

where r is the separation between the Q and \bar{Q} . The parameters are $\sigma = 0.192$ GeV², $\alpha = 0.471$, $m_c = 1.32$ GeV and $m_b = 4.746$ GeV [14]. This potential is modified at finite temperatures due to color screening, becoming

$$V(r, T) = \frac{\sigma}{\mu(T)}(1 - e^{-\mu(T)r}) - \frac{\alpha}{r}e^{-\mu(T)r}. \quad (3)$$

The screening mass, $\mu(T)$, is an increasing function of temperature. When $\mu(T = 0) \rightarrow 0$, eq. (2) is recovered. At finite temperature, when $r \rightarrow 0$, the $1/r$ behavior is dominant while as $r \rightarrow \infty$ one finds that the range of the potential decreases with $\mu(T)$, making the binding less effective at finite temperature. Semiclassically the energy is

$$E(r, T) = 2m_Q + \frac{c}{m_Q r^2} + V(r, T) , \quad (4)$$

where $\langle p^2 \rangle \langle r^2 \rangle = c \approx \mathcal{O}(1)$ [14]. Minimizing $E(r, T)$ gives the radius of the bound state at each T . For $\mu(T)$ above a certain critical value, μ_D , there is no longer a minimum and the screening has become strong enough for binding to be impossible and the resonance no longer forms in the plasma. The temperature T_D at which this happens is that for which $\mu(T_D) = \mu_D$.

The values of μ_D for the bottomonium states are given in Table 2, along with the bottomonium mass at $\mu = \mu_D$, $M(\mu_D)$. Also shown are the results for the charmonium states. We note that μ_D and $M(\mu_D)$ are independent of T_D , but that T_D depends upon the functional form of $\mu(T)$. Table 2 shows that the Υ mass is actually larger at breakup than at $T = 0$ because the $1/r$ contribution to the potential is dominant, whereas the Υ' and $\chi_b(1P)$ masses are smaller due to the fact that the linear term is more important for these resonances.

	Υ	Υ'	$\chi_b(1P)$	J/ψ	ψ'	$\chi_c(1P)$
M (GeV)	9.445	10.004	9.897	3.07	3.698	3.5
r (fm)	0.226	0.509	0.408	0.453	0.875	0.696
τ_F (fm)	0.76	1.9	2.6	0.89	1.5	2.0
$M(\mu_D)$ (GeV)	9.615	9.778	9.829	2.915	3.177	3.198
μ_D (GeV)	1.565	0.671	0.558	0.699	0.357	0.342

Table 2: Properties of the quarkonium states both at zero temperature and at $T = T_D$ (the breakup temperature for each bound state), taken from Ref. [14]. The masses at $T = 0$ are from the solution to the Schrodinger equation with the potential of eq. (2). Note that r is the distance between the Q and \bar{Q} and τ_F is the formation time of the bound state. $M(\mu_D)$ and μ_D are the mass at breakup and the screening mass at T_D ; both are independent of the actual value of T_D as determined by the functional form of $\mu(T)$.

It is necessary to know the dependence of the screening mass on temperature before the breakup temperature T_D can be determined. Since the behavior of $\mu(T)$ is unknown for $T \gg T_c$, we consider two scenarios which may be expected to bracket the realistic situation.

- The first is a parameterization based on $SU(N)$ lattice simulations [23],

$$\frac{\mu(T)}{T_c} \simeq 4 \frac{T}{T_c} \quad (5)$$

which results in the lowest values of T_D . Although this parameterization of $\mu(T)$ is independent of T_c , we will present our results as a function of the ratio T/T_c taking $T_c = 260$ MeV, consistent with $SU(3)$ lattice calculations. For this value of T_c , the Υ breaks up at $T_D/T_c \approx 1.5$. In Ref. [22], this parameterization was used with $T_c = 150$ MeV, leading to the estimate $T_D/T_c \sim 2.6$ for the Υ .

- The second is an estimate from perturbation theory [24],

$$\frac{\mu(T)}{T_c} = \sqrt{1 + \frac{n_f}{6}} g \left(\frac{T}{T_c} \right) \frac{T}{T_c}, \quad (6)$$

where the temperature-dependent running coupling constant is

$$g^2 \left(\frac{T}{T_c} \right) = \frac{24\pi^2}{(33 - 2n_f) \ln[(19T_c/\Lambda_{\overline{\text{MS}}})(T/T_c)]}. \quad (7)$$

In $SU(3)$ gauge theory, $T_c/\Lambda_{\overline{\text{MS}}} = 1.78 \pm 0.03$ [14]. In this case, T_D can be quite high and depends strongly on n_f and T_c . We present results using eq. (6) with $n_f = 3$ and $T_c = 150$ MeV.

We shall refer to these two distinct choices for $\mu(T)$ as the $SU(N)$ and 3-Flavor QGP's, respectively. The temperature dependence for both estimates of $\mu(T)$ is shown in Fig. 1 with μ_D indicated for Υ , Υ' and χ_b . The values of T_D are given in Table 3 for both cases. Even in the first case, the early estimates of initial temperatures of order $T_0 \sim 260$ MeV for the LHC implied that Υ suppression would be unlikely [12], and that even Υ' and χ_b suppression would not be certain.

In contrast, the higher ‘minijet’ value of $T_0 \sim 1.14$ GeV, combined with the results of Fig. 1 and the T_D values given in Table 3 indicate that, when the $SU(N)$ parameterization is used, the Υ may easily be suppressed in the minijet gluon plasma at LHC energies. However, the 3-Flavor estimate leads to much higher breakup temperatures for the Upsilon states and the distinct possibility that the Υ will not be suppressed³ even though the Υ' and χ_b could be suppressed. In either case, the suppression pattern depends on the space-time evolution of the plasma. Depending upon circumstances, this dependence could be either an impediment to the extraction of the physics of

³Note that Υ production from Υ' and χ_b decays will be suppressed if the Υ' and χ_b states are suppressed.

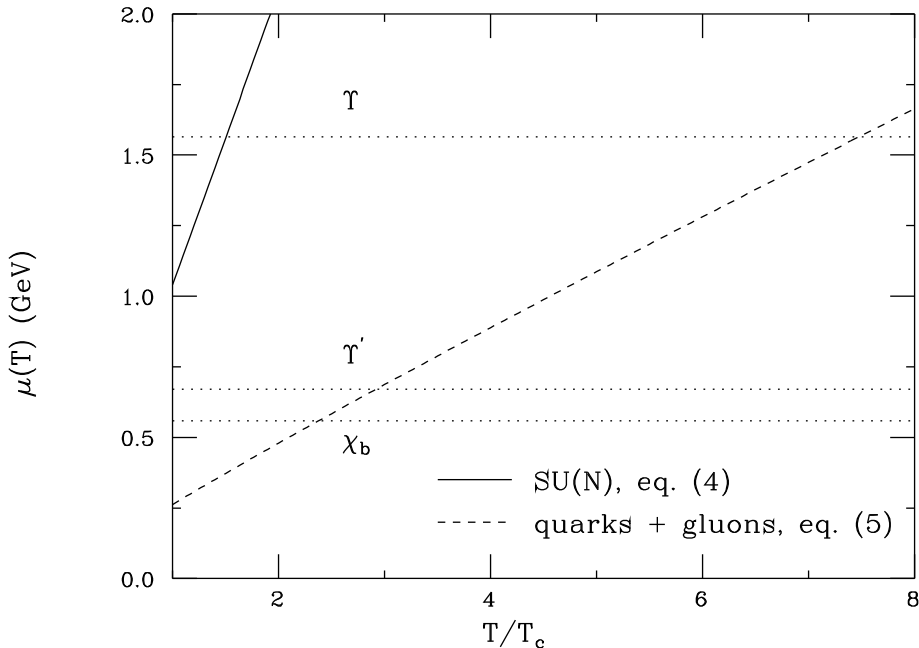


Figure 1: The screening mass as a function of temperature for the scenarios of eqs. (5) (solid) and (6) (dashed). The values of μ_D at breakup for the Υ , Υ' , and χ_b are also indicated by the dotted lines.

the QGP or a very powerful tool. In most scenarios, much can be learned about the QGP by simply examining the ratio [22] of production rates for higher $b\bar{b}$ resonances to the production rate for the Υ . However, for a quantitative determination of QGP suppression on an absolute scale, a benchmark such as Z production, to which Υ production cross sections may be compared, is needed.

3 Cross sections, rates, and the color evaporation model

Before turning to the details of Υ suppression, let us determine whether or not the Υ production rate is large enough for any suppression to be observable. An estimate of the Υ yield is not straightforward since the formation of bound states from the predominantly color octet $Q\bar{Q}$ pairs is nonperturbative and therefore model-dependent.

The color evaporation model [25] has often been applied to the production of quarkonium states below the open charm/bottom thresholds. The $Q\bar{Q}$ pair neutralizes its color by interaction with the collision-induced color field—

T_D (MeV)		
	SU(N) only, eq. (5)	gluons and quarks, eq. (6)
Υ	391	1125
Υ'	260	447
χ_b	260	368
J/ψ	260	459
ψ'	260	211.5
χ_c	260	204

Table 3: The values of T_D (in MeV) for the two choices of $\mu(T)$, eq. (5) and eq. (6). We employ $T_c = 260$ MeV for the SU(N) case and $T_c = 150$ MeV in the case of eq. (6). The lower T_c used in the 3-Flavor case results in the lower T_D values for the ψ' and χ_c .

“color evaporation”. The Q and the \bar{Q} either combine with light quarks to produce heavy-flavored hadrons or bind with each other in a quarkonium state. The additional energy needed to produce heavy-flavored hadrons is obtained nonperturbatively from the color field in the interaction region. Depending on m_Q , the yield of all quarkonium states may be only a small fraction of the total $Q\bar{Q}$ cross section below the $\sqrt{\hat{s}} = 2m_H$ threshold, where m_H is the mass of the lightest heavy-flavored meson. The total heavy quark cross section below this $H\bar{H}$ threshold, $\tilde{\sigma}$, is calculated at leading order by integrating over the $Q\bar{Q}$ pair mass from $2m_Q$ to $2m_H$,

$$\tilde{\sigma}(s) = \sum_{i,j} \int_{4m_Q^2}^{4m_H^2} d\hat{s} \int dx_1 dx_2 f_{i/p}(x_1) f_{j/p}(x_2) \sigma_{ij}(\hat{s}) \delta(\hat{s} - x_1 x_2 s), \quad (8)$$

where $ij = q\bar{q}$ or gg and $\sigma_{ij}(\hat{s})$ is the $ij \rightarrow Q\bar{Q}$ subprocess cross section. The color evaporation model was taken to next-to-leading order (NLO) using the exclusive $Q\bar{Q}$ hadroproduction calculation [26] to obtain the energy, x_F , and p_T -dependence of quarkonium production [27, 28].

The division of $\tilde{\sigma}$ into heavy flavored hadrons vs. quarkonium and the relative quarkonium production rates are both a matter of assumption in the color evaporation model. For the model to have any predictive power, the relative quarkonium production rates should be independent of projectile, target, and energy. Experiment suggests that this is true for the charmonium ratios χ_c/ψ and ψ'/ψ over a broad energy range [29, 30, 31, 32]. The available bottomonium data follows this trend: $\Upsilon'/\Upsilon = 0.53 \pm 0.13$ and $\Upsilon''/\Upsilon = 0.17 \pm 0.06$ for proton beams at 400 [33] and 800 GeV [34, 35]. These results are consistent with the production of Υ states in $p\bar{p}$ collisions at the Tevatron [36]. The color evaporation model also reproduces the energy dependence

of charmonium and bottomonium production over a wide range of energy as well as most of the x_F dependence of the charmonium states⁴, provided the fraction of quarkonium vs. $H\bar{H}$ states is assumed to be independent of all kinematic variables.

With these assumptions and our knowledge of the Υ'/Υ and Υ''/Υ ratios at low energy, the normalization of each quarkonium state can be fixed empirically from data, allowing predictions of the production cross sections at LHC energies. The procedure we have followed is described below.

- As a first step, we assess the accuracy of the model for describing existing $pp/p\bar{p}$ data. Fixed target Υ data has been generally given as the sum of Υ , Υ' , and Υ'' production. From this data, one can determine $B(d\sigma/dy)_{y=0}$ where B is an effective dilepton branching ratio reflecting the production yield through the Υ , Υ' , and Υ'' resonances. As shown in Fig. 2, taken from Ref. [27], a good fit to the data, up to and including ISR energies [33, 34, 35, 38, 39], is obtained with

$$B \left(\frac{d\sigma(s)}{dy} \right)_{y=0} = 1.6 \times 10^{-3} \left(\frac{d\tilde{\sigma}(s)}{dy} \right)_{y=0}, \quad (9)$$

where $d\tilde{\sigma}/dy$ is computed using the MRS D- $'$ [6] or GRV HO [40] PDFs, taking $m_b = 4.75$ GeV and the renormalization and factorization scales set to $\mu = m_{T,b\bar{b}} = \sqrt{m_b^2 + (p_{T,b}^2 + p_{T,\bar{b}}^2)/2}$. The high energy data from UA1 [41] and CDF [36] are also shown in Fig. 2 and agree very well with the energy dependence of the color evaporation model, as obtained from eq. (8). Both sets of PDFs give compatible predictions at the LHC energy. The predicted cross section is up to a factor of 20 larger at 5.5 TeV than that given by the empirical parameterization, $d\sigma/dy|_{y=0} \propto \exp(-14.7M_\Upsilon/\sqrt{s})$ [42, 43], labeled CR in Fig. 2.

- The second step is to extract the Υ , Υ' and Υ'' components separately using the Υ'/Υ and Υ''/Υ ratios quoted earlier, and the known branching ratios $B_{\Upsilon_i} \equiv B(\Upsilon_i \rightarrow \mu^+\mu^-)$ where Υ_i represents the individual Υ states. If we write $d\sigma_{\Upsilon_i}/dy|_{y=0} \equiv f_{\Upsilon_i}d\tilde{\sigma}/dy|_{y=0}$ for the Υ_i cross sections, then from eq. (9)

$$f_\Upsilon B_\Upsilon + f_{\Upsilon'} B_{\Upsilon'} + f_{\Upsilon''} B_{\Upsilon''} = B = 0.0016. \quad (10)$$

Using $f_{\Upsilon'}/f_\Upsilon = 0.53$ and $f_{\Upsilon''}/f_\Upsilon = 0.17$, as quoted earlier, and B_{Υ_i} from the Particle Data Book [44], we find [28]

$$f_\Upsilon = 0.044, \quad f_{\Upsilon'} = 0.023, \quad f_{\Upsilon''} = 0.0074. \quad (11)$$

⁴At high x_F , additional production from other mechanisms such as intrinsic heavy quarks [37] may be important.

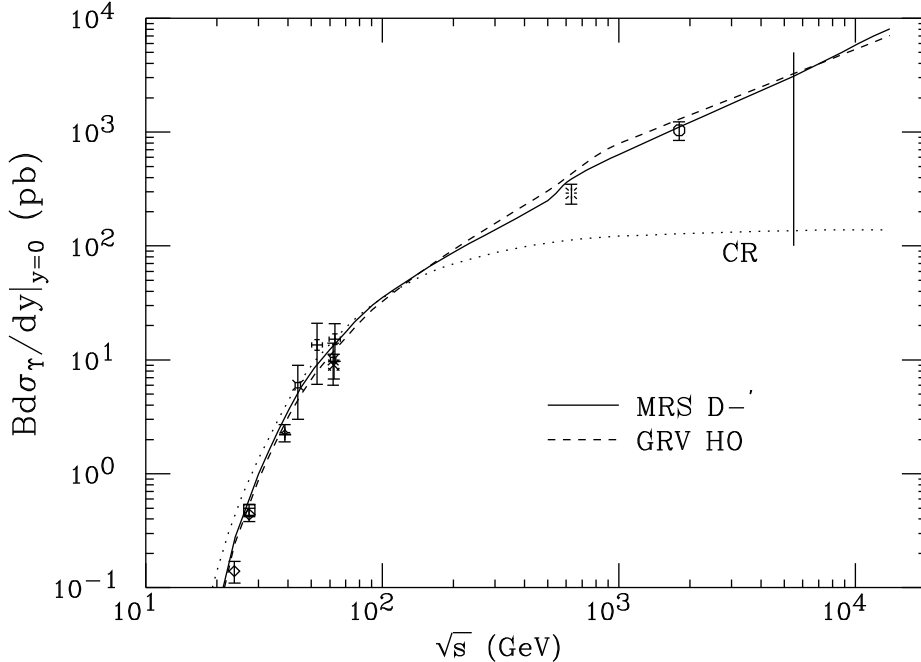


Figure 2: We show $Bd\sigma/dy|_{y=0}$ for $\Upsilon + \Upsilon' + \Upsilon''$ in pp collisions, as indicated in eq. (9), for the MRS D-’ [6] (solid) and GRV HO [40] (dashed) parton densities. Also shown is the empirical Craigie parameterization [42, 43] (dotted). The data are taken from [33, 34, 36, 38, 39, 41]. The vertical solid line indicates the maximum LHC Pb+Pb energy. This figure was first presented in Ref. [27].

- Thirdly, we must separate direct from indirect production. The measured Υ_i production cross sections, or equivalently the f_{Υ_i} , are only effective values which reflect both direct production and chain decays of higher mass states. Isolation of the direct production cross sections for each Υ_i requires detection of the radiated photons associated with chain decays. Data which allows this separation is not currently available. As discussed later, the extent to which the required photon detection will be possible at the LHC is also uncertain. We shall see that this is a very important issue. For now, we make the assumptions:

$$f_{\chi_{bi}(1P)}^d = f_{\Upsilon'}; \quad f_{\chi_{bi}(2P)}^d = f_{\Upsilon''}, \quad (12)$$

for *each* i , where $i = 0, 1, 2$ labels the χ_b states in PDG notation [44], and the d superscript indicates the f for *direct* production. With this and the summed branching ratios [44]

$$\sum_{i=0,1,2} B(\chi_{bi}(1P) \rightarrow \Upsilon\gamma) \sim 0.63,$$

$$\begin{aligned}\sum_{i=0,1,2} B(\chi_{bi}(2P) \rightarrow \Upsilon\gamma) &\sim 0.16, \\ \sum_{i=0,1,2} B(\chi_{bi}(2P) \rightarrow \Upsilon'\gamma) &\sim 0.42,\end{aligned}$$

along with $B(\Upsilon' \rightarrow \Upsilon X) \sim 0.27$ and Υ'' decays to Υ' , Υ and $\chi_{bi}(2P)$, we can compute the f^d 's for direct production of all the Υ_i . One finds that about 0.014 of the total $f_\Upsilon = 0.044$ is due to $\chi_{bi}(1P)$ decays. This would be similar to what is found in the analogous ψ , χ_c situation. Similarly, ~ 0.001 of f_Υ and ~ 0.003 of $f_{\Upsilon'}$ would be due to $\chi_{bi}(2P)$ decays. Also important are $\Upsilon' \rightarrow \Upsilon X$ decays; $f_{\Upsilon'}$ [eq. (11)] implies that an additional 0.006 of f_Υ would be indirect. The contributions from chain decays of the Υ'' are small. Also, there are no contributions to the Υ'' rate coming from higher states that are known to be significant. Altogether, we would have:

$$\begin{aligned}f_\Upsilon^d &\sim 0.023, \quad f_{\Upsilon'}^d \sim 0.020, \quad f_{\Upsilon''}^d \sim 0.0074, \\ f_{\chi_{bi}(1P)}^d &\sim 0.023, \quad f_{\chi_{bi}(2P)}^d \sim 0.0074,\end{aligned}\tag{13}$$

where $i = 0, 1, 2$ labels the different $\chi_{bi}(1P, 2P)$ states. Note that only about half of f_Υ is due to direct Υ production. The results in eq. (13) imply that about 14% of $\tilde{\sigma}$ goes into bottomonium state production.

In Table 4, we give the corresponding normalized direct production cross sections in pp collisions, $f^d\tilde{\sigma}$, for each state with f^d from eq. (13) and $\tilde{\sigma}$ computed using the MRS D-' parton densities at 5.5 TeV. The cross sections given in Table 4 are integrated over all rapidity. At this energy, the results with the GRV HO distributions are about 20% smaller.

We would like to comment on the differences between the color evaporation model used here and other models of quarkonium production. The color singlet model [45], in which bound states with the right quantum numbers are directly produced, has been shown to be insufficient to reproduce the Tevatron data on J/ψ , ψ' , and Υ production [29, 36]. The low- p_T Υ production data from the Tevatron has recently been explained using a model of color octet production involving corrections to the bound state wavefunctions at higher order in the relative velocity of the $Q\bar{Q}$ where $\alpha_s \sim v$ for the bound state [46]. We would like to point out that the p_T -dependence of quarkonium production is quite similar to the p_T -dependence of unbound $Q\bar{Q}$ pairs [26]. This same dependence also appears in the color octet model since the octet mechanism makes other 3S_1 production channels available. Thus the color octet model is quite similar in spirit to the color evaporation model considered here. However, at larger p_T , $p_T > m_\Upsilon$, fragmentation processes such as $g \rightarrow \Upsilon$ and $b \rightarrow \Upsilon$ [47] should eventually dominate the production processes considered in the color octet model. It has been recently shown that

	Υ	Υ'	Υ''	$\chi_b(1P)$	$\chi_b(2P)$
$f^d \tilde{\sigma}$ (nb)	426	233	137	426	137
$N^d(\text{PbPb})$	2.02×10^6	1.75×10^6	6.47×10^5	2.02×10^6	6.47×10^5
$N_{\mu\mu}^d(\text{PbPb})$	4.99×10^4	2.30×10^4	1.17×10^4	-	-

Table 4: The normalized cross sections, $f^d \tilde{\sigma}$, for directly produced bottomonium states in pp collisions at 5.5 TeV, using the f^d 's of eq. (13) and the prediction of eq. (8) that $\tilde{\sigma} = 17.35 \mu\text{b}$ [27], where the MRS D-' parton densities are employed with $m_b = 4.75$ GeV and $\mu = m_{T, b\bar{b}}$. Also given is the number N^d of each type of bottomonium state produced directly in Pb+Pb collisions at the LHC, calculated using eq. (14) with $\sigma_{NN} = 60$ mb, $T_{\text{PbPb}}(\mathbf{0}) = 32 \text{ mb}^{-1}$ and $L_{\text{int}}^{\text{PbPb}} = 2.59 \text{ nb}^{-1}$. For $\Upsilon, \Upsilon', \Upsilon''$ we give the corresponding number of $\mu^+ \mu^-$ pairs from decay of directly produced states.

the Tevatron charmonium and bottomonium p_T data is also in good agreement with the color evaporation model at NLO, as described in [28]. In the color evaporation picture, gg scattering followed by the splitting $g \rightarrow b\bar{b}$ incorporated at NLO is similar to models of $g \rightarrow \Upsilon$ fragmentation [47]. By including this splitting, the color evaporation model provides a good description of the quarkonium p_T distributions.

We can now employ the results for f^d given in Table 4 to predict rates for direct production of bottomonium states in Pb+Pb collisions at the LHC. For central collisions, the expected rates are given by

$$N^d = \sigma_{NN} T_{\text{PbPb}}(\mathbf{0}) f^d \tilde{\sigma} L_{\text{int}}^{\text{PbPb}}, \quad (14)$$

where $\sigma_{NN} T_{\text{PbPb}}(\mathbf{0})$ is the number of central Pb+Pb collisions⁵ and $f^d \tilde{\sigma}$, with f^d taken from eq. (13), is the cross section for direct production of a given bottomonium state in pp collisions. In one month of running the integrated luminosity for lead beams is expected to be $L_{\text{int}}^{\text{PbPb}} = 2.59/\text{nb}$. Typical rates are given in Table 4; they are on the order of 10^6 for Υ and Υ' . Approximately 10-15% of the cross section is within $|\eta| \leq 1$. The number of muon pairs from the Υ, Υ' and Υ'' decays, found by multiplying the total number of Υ_i directly produced, N^d , by the appropriate branching ratio, is also given in Table 4. These rates suggest that production and suppression of these states should be measurable by CMS in the very clean $\mu^+ \mu^-$ final state decay mode. The rapidity distributions are rather broad and nearly constant out to $y \simeq 4$ with the MRS D-' parton distributions. The GRV HO results exhibit a somewhat narrower rapidity plateau [27].

⁵We use $\sigma_{NN} \approx 60$ mb, assuming that the high energy rise in $\sigma_{p\bar{p}}$ will also hold for σ_{NN} , and $T_{\text{PbPb}}(\mathbf{0}) \simeq 32/\text{mb}$.

The rates of Table 4 are those obtained by simply multiplying the pp cross section by the expected number of central Pb+Pb collisions. This procedure does not include any nuclear effects (*e.g.* shadowing or absorption) on Υ production. However, significant nuclear effects have been observed in fixed-target interactions. The E772 collaboration has measured a less than linear A dependence for Υ production at $\sqrt{s} = 38.8$ GeV, $\sigma_{pA}^{\Upsilon} = \sigma_{pp}^{\Upsilon} A^{\alpha}$ where $\alpha = 0.96$ [48]. If no nuclear effects were present, the production cross section would grow as A^1 . Note that $\alpha = 0.96$ implies a 20% reduction in the p Pb production cross section relative to the A^1 prediction. The two possible sources of this reduction in pA collisions are shadowing and absorption.

- If the reduction is due to shadowing, the observed greater suppression (smaller α) of J/ψ compared to Υ implies that the shadowing of the gluon PDFs is greater at smaller x values. This would then imply that, for the Υ (or any other given onium resonance), shadowing would be greater at higher energies due to the lower x region probed. In heavy-ion collisions at LHC energies the shadowing mechanism could reduce $\sigma_{\text{PbPb}}^{\Upsilon}$ by 25-40% relative to the result obtained assuming proportionality to A^2 [49]. The larger shadowing effect expected for Pb+Pb collisions compared to p Pb collisions comes from the convolution of two nuclei with modified parton densities. To the extent that shadowing in central collisions is the same as for minimum bias collisions (which include peripheral as well as central collisions), the same 25-40% reduction should be applied to the numbers of Table 4. However, nucleons near the nuclear surface might experience a smaller shadowing effect than those in the center of the nucleus.
- On the other hand, the deviation of the A dependence from unity in fixed-target interactions has also been attributed to absorption by nucleons; interactions with comoving secondaries are possible although rare in pA collisions. In this approach, α is related to the effective onium absorption cross section in nuclear matter by $1 - \alpha \approx 9\sigma_{\text{abs}}/16\pi r_0^2$, assuming a step function nuclear shape. The apparent Υ absorption cross section is 40-50% less than the ψ absorption cross section, suggesting that the Υ suffers fewer final-state interactions than the J/ψ (possibly because of its smaller size). The onium-nucleon absorption cross section has been calculated on the basis of the operator-product expansion [50, 51] and has been shown to quickly attain its asymptotic value [52]. Absorption by nucleons has been shown to be less effective in peripheral relative to central nuclear collisions, see *e.g.* [18, 20]. Therefore nucleon interactions with the J/ψ may be insufficient to account for J/ψ measurements in heavy-ion interactions at current energies [15, 16]. Secondary particle production increases in

central relative to peripheral collisions, increasing the influence of comovers in central collisions as well as in nuclear collisions compared to pA interactions [20]. The onium-comover cross section can be estimated from the onium-nucleon absorption cross section by the additive quark model assuming the comovers are mesons [53].

A mixture of shadowing and absorption is most likely. If the value of α depends on the Upsilon state, absorption is important: σ_{abs} could increase with the size of the Upsilon state [54]. If shadowing were dominant, α would remain essentially unchanged since the x values probed by the different Upsilon states are very nearly equal. In fact, the E772 collaboration observed no difference in the J/ψ and ψ' A dependence or in the Υ and Υ' A dependence within their uncertainties [48]. Additionally the ψ'/ψ ratio appears to be independent of A [27] but the data is such that a size-dependence of the absorption cross section cannot be ruled out. At the E772 energy, $\sqrt{s} = 38.8$ GeV, the target momentum fractions probed are $x \leq 0.08$ for the charmonium states, just in the shadowing region, while for the Υ states, $x \leq 0.25$, in the EMC or antishadowing regions. At the lower energies of other J/ψ measurements, shadowing should be less effective than absorption [55]. The mass scale in the PDF is also important if the shadowing is Q^2 dependent [56]. In Q^2 -dependent shadowing models, the gluon distribution evolves fastest with Q^2 ; the valence and sea quark evolution is rather weak for $2 < Q^2 < 10$ GeV² [49, 56]. We note that nuclear deep-inelastic scattering data do not exhibit strong Q^2 dependence for $Q^2 \leq 100$ GeV² [57], in agreement with these models, but it is more difficult to probe the Q^2 dependence of gluon shadowing. Precision pA data is needed to sort out these effects, particularly at higher than current energies since at RHIC and LHC we will be in a new regime where x is small and Q^2 is relatively large. Measurements of dilepton production will prove helpful, as we discuss later, since the dilepton continuum could be influenced by shadowing but not by absorption.

The p_T -dependence of the suppression from shadowing/absorption is especially crucial for our later considerations. Since pA studies are not possible at the LHC, the exact rapidity and p_T -dependence of shadowing/absorption suppression at the low x values probed at 5.5 TeV will be imprecisely known. Thus, it is fortunate that the p_T -dependence of such suppression should be much weaker than that from QGP suppression (as we shall discuss below). As noted above, if shadowing is dominant, then suppression from this purely nuclear source should also be essentially independent of the Upsilon state. As our ensuing discussion will show, this would be a very important advantage. In contrast, if absorption is dominant the magnitude of the suppression could depend on the Upsilon state. Finally, we note that any broadening of the p_T -dependence due to initial-state interactions in the nuclear target [58] may be expected to be negligible. Thus, we believe that any alteration of the

p_T -spectra for the various members of the Υ family due to QGP effects will stand out clearly. Even more crucially, in the absence of QGP suppression the ratios of rates for different Υ family members should exhibit p_T dependence that is precisely that predicted without including shadowing or absorption.⁶ *The p_T -dependence for such ratios is then a direct probe of the QGP physics.*

4 Sensitivity of quarkonium suppression to the QGP model

As we have just shown, the Υ production rate is high enough at the LHC for any QGP effects on the Υ family to be measurable. Our discussion in Sec. 2 suggested that at the high temperatures predicted for the minijet plasma, Υ production may be suppressed at the LHC. We would like to use this suppression to determine the initial conditions of the QGP, including T_0 , t_0 , and the temperature dependence of the QGP screening mass $\mu(T)$. A simple measurement of the overall suppression of the production rates for the Upsilon family members will not be adequate. We must consider additional observables that could be affected by the presence of the QGP. In this section, we will show that the p_T -dependence of the suppression provides a remarkable amount of information.

If the QGP were of infinite temporal and spatial extent, resonance production would be suppressed as long as $T > T_D$. But, there would be no significant p_T -dependence. In fact, however, both the lifetime and the spatial extent of the QGP are finite. Since a color singlet $Q\bar{Q}$ pair takes some time to form a bound state, the competition between the formation time, the time needed for the $Q\bar{Q}$ to separate to the bound state radius⁷, and the characteristics of the plasma all affect the p_T -dependence of the Υ states. We will now discuss the sensitivity of the onium suppression patterns as a function of p_T to these ingredients.

The finite lifetime of the plasma sets an upper limit on the p_T at which the onium states can be suppressed. In the plasma rest frame, the $b\bar{b}$ forms a bound state in the time $t_F = \gamma\tau_F$ where $\gamma = \sqrt{1 + (p_T/M)^2}$ (M is the onium mass) and the formation times, τ_F , for the bottonium and charmonium states were given in Table 2. When the plasma has cooled below T_D , the production of the bound state is no longer suppressed. The time at which this occurs can be determined from the Bjorken model [59] which assumes that the evolution of the system is described by ideal hydrodynamics, cooling by an isentropic

⁶If absorption is significant and σ_{abs} depends upon the Upsilon state, then the ratio of p_T -integrated cross sections would be affected but not the p_T variation.

⁷If the $Q\bar{Q}$ is produced as a color octet, it is less likely to produce quarkonium than heavy-flavored hadrons.

expansion so that

$$s_D t_D = s_0 t_0 . \quad (15)$$

Since the entropy density, s , is proportional to T^3 , the time at which the temperature drops below T_D is

$$t_D = t_0 \left(\frac{T_0}{T_D} \right)^3 . \quad (16)$$

As long as $t_D/t_F > 1$, quarkonium formation will be suppressed. Thus the maximum p_T at which suppression occurs is

$$p_{T,\max} = M \sqrt{(t_D/\tau_F)^2 - 1} . \quad (17)$$

The values for t_D and $p_{T,\max}$ for all the onium states are given in Tables 5 and 6 for both forms of $\mu(T)$, eqs. (5) and (6), and three different sets of initial conditions for LHC and RHIC energies.

It is easy to check whether or not the bottomonium states are suppressed given the formation time and T_0 from the minijet initial conditions. The $SU(N)$ parameterization of eq. (5), with $T_c = 260$ MeV, results in $t_D/\tau_F > 1$ for all the members of the Upsilon family. Thus, all the states will be suppressed up to rather large values of p_T , suggesting that any suppression should be easily observable within the p_T acceptance of CMS. However, T_0 is reduced to 900 MeV when quark degrees of freedom are added as in the 3-Flavor scenario of eq. (6); the result is that $t_D/\tau_F < 1$ for all the bottomonium states and no suppression occurs. In other words, if the 3-Flavor quark-gluon plasma is finite and quickly equilibrated, none of the Υ states will be suppressed, and the p_T -dependence should be unchanged from pp production modulo any nuclear effects on Υ production.

In contrast, the charmonium states are suppressed in both the $SU(N)$ and the 3-Flavor $\mu(T)$ scenarios. The $SU(N)$ case gives values of $p_{T,\max}$ similar to or smaller than those of the bottomonium family because of the smaller charmonium masses. This should be contrasted with the 3-Flavor QGP for which the J/ψ would be suppressed over a very narrow range of p_T relative to the χ_c and ψ' since the value of T_D for the J/ψ is nearly twice that of the other charmonium states (see Table 3 for T_D). If the p_T -dependence of the nuclear effects on the charmonium states is weak, then the ratio of higher charmonium states to the J/ψ as a function of p_T would still be useful.

We discuss the other initial conditions shown in Tables 5 and 6 and their consequences later.

In a finite system, such as those produced in heavy-ion collisions, the suppression also depends on the size of the system. We present a schematic

LHC				
SU(N) only, eq. (5)		gluons and quarks, eq. (6)		
minijet initial conditions				
$T_0 = 1.14$ GeV, $t_0 = 0.1$ fm		$T_0 = 900$ MeV, $t_0 = 0.1$ fm		
	t_D (fm)	$p_{T,\max}$ (GeV)	t_D (fm)	$p_{T,\max}$ (GeV)
Υ	2.49	29.5	0.105	0
Υ'	8.474	43.5	1.67	0
χ_b	8.474	30.7	1.46	0
ψ	8.474	29.0	1.54	4.34
ψ'	8.474	20.6	15.7	38.6
χ_c	8.474	14.4	17.5	30.5
Uncertainty relation initial conditions				
$C = 1$				
$T_0 = 600$ MeV, $t_0 = 0.11$ fm		$T_0 = 785$ MeV, $t_0 = 0.084$ fm		
$C = 3$				
$T_0 = 346$ MeV, $t_0 = 0.57$ fm		$T_0 = 453$ MeV, $t_0 = 0.436$ fm		
	t_D (fm)	$p_{T,\max}$ (GeV)	t_D (fm)	$p_{T,\max}$ (GeV)
Υ	0.39	0	0.03	0
Υ'	1.3	0	0.455	0
χ_b	1.3	0	0.82	0
ψ	1.3	3.27	0.42	0
ψ'	1.3	0	4.28	9.9
χ_c	1.3	0	4.78	7.6
parton gas initial conditions				
$T_0 = 820$ MeV, $t_0 = 0.5$ fm		$T_0 = 820$ MeV, $t_0 = 0.5$ fm		
	t_D (fm)	$p_{T,\max}$ (GeV)	t_D (fm)	$p_{T,\max}$ (GeV)
Υ	4.6	56.53	0.19	0
Υ'	15.69	81.98	3.09	12.83
χ_b	15.69	58.9	5.53	18.58
ψ	15.69	54.0	2.85	9.34
ψ'	15.69	38.5	29.1	71.6
χ_c	15.69	27.2	32.5	56.76

Table 5: LHC values of t_D , and $p_{T,\max}$ for the two choices, eq. (5) and eq. (6), of $\mu(T)$, and for three sets of initial conditions.

RHIC				
	SU(N) only, eq. (5)		gluons and quarks, eq. (6)	
minijet initial conditions				
	$T_0 = 445$ MeV, $t_0 = 0.1$ fm		$T_0 = 360$ MeV, $t_0 = 0.1$ fm	
	t_D (fm)	$p_{T,\max}$ (GeV)	t_D (fm)	$p_{T,\max}$ (GeV)
Υ	0.15	0	0.003	0
Υ'	0.5	0	0.05	0
χ_b	0.5	0	0.094	0
ψ	0.5	0	0.048	0
ψ'	0.5	0	0.493	0
χ_c	0.5	0	0.55	0
Uncertainty relation initial conditions				
$C = 1$				
	$T_0 = 400$ MeV, $t_0 = 0.164$ fm		$T_0 = 524$ MeV, $t_0 = 0.126$ fm	
$C = 3$				
	$T_0 = 231$ MeV, $t_0 = 0.85$ fm		$T_0 = 303$ MeV, $t_0 = 0.65$ fm	
	t_D (fm)	$p_{T,\max}$ (GeV)	t_D (fm)	$p_{T,\max}$ (GeV)
Υ	0.17	0	0.013	0
Υ'	0.59	0	0.2	0
χ_b	0.59	0	0.364	0
ψ	0.59	0	0.188	0
ψ'	0.59	0	1.92	2.94
χ_c	0.59	0	2.14	1.31
parton gas initial conditions				
	$T_0 = 550$ MeV, $t_0 = 0.7$ fm		$T_0 = 550$ MeV, $t_0 = 0.7$ fm	
	t_D (fm)	$p_{T,\max}$ (GeV)	t_D (fm)	$p_{T,\max}$ (GeV)
Υ	1.95	22.3	0.082	0
Υ'	6.63	33.4	1.3	0
χ_b	6.63	23.2	2.33	0
ψ	6.63	22.6	1.2	2.8
ψ'	6.63	15.9	12.3	30.12
χ_c	6.63	11.1	13.7	23.75

Table 6: RHIC values of t_D , and $p_{T,\max}$ for the two choices, eq. (5) and eq. (6), of $\mu(T)$, and for three sets of initial conditions.

calculation of the p_T -dependence of the suppression following Ref. [60]. Similar analyses of QGP production have also been done [22, 61, 62]. We can assume that the initial entropy profile is dependent on the radius of the QGP,

$$s_0(r) = s_0 \left(1 - \left(\frac{r}{R} \right)^2 \right)^\beta, \quad (18)$$

so that

$$t_D(r) = t_D(0) \left(1 - \left(\frac{r}{R} \right)^2 \right)^\beta, \quad (19)$$

where $t_D(0)$ is the value of t_D calculated in eq. (16) for resonances produced in the center of the system and R is the transverse radius of the plasma, assumed to be no larger than the radius of the nucleus, $R \simeq 1.2A^{1/3}$. At any time t during the evolution of the QGP, the spatial boundary of the screening region is located at the transverse radius r_S given by $t_D(r_S) = t$,

$$r_S = R \left(1 - \left(\frac{t}{t_D(0)} \right)^{1/\beta} \right)^{1/2}. \quad (20)$$

In general, if the $Q\bar{Q}$ pair is created with transverse position $x^\mu = (0, \mathbf{r}, 0)$ and momentum $p^\mu = (\sqrt{M^2 + p_T^2}, \mathbf{p}_T, 0)$, at the formation time τ_F the pair will form a bound state at $x^\mu = (\tau_F \sqrt{1 + (p_T/M)^2}, \mathbf{r} + \tau_F \mathbf{p}_T/M, 0)$. If $|\mathbf{r} + \tau_F \mathbf{p}_T/M| \geq r_S$, the $Q\bar{Q}$ pair escapes the QGP before τ_F and will successfully form bound states. This inequality will be satisfied (and the pairs will escape) for a range of angles between \mathbf{r} and \mathbf{p}_T — $0 \leq \theta \leq \theta_{\max}(r, p_T)$ — provided p_T is such that $(r + \tau_F p_T/M) > r_S$. Here, θ_{\max} also depends on τ_F , M , and r_S as detailed below. The p_T -dependent probability that the $Q\bar{Q}$ pair survives and is able to form an onium state, $S(p_T)$, is the ratio of the number of bound states produced by those pairs that escape the plasma to the maximum possible number of onium bound states that would be formed at the given p_T in the absence of the QGP:

$$S(p_T) = \frac{\int_0^R dr r \rho(r) \theta(r, p_T)}{\pi \int_0^R dr r \rho(r)}, \quad (21)$$

where we parameterize $\rho(r) = (1 - (r/R)^2)^\alpha$ and

$$\theta(r, p_T) = \begin{cases} \pi & z \leq -1 \\ \cos^{-1} z & |z| < 1 \\ 0 & z \geq 1 \end{cases}, \quad (22)$$

where

$$z = \frac{r_S^2 - r^2 - \left(\frac{\tau_F p_T}{M}\right)^2}{2\tau_F r \frac{p_T}{M}}. \quad (23)$$

When $z \geq 1$ the pair cannot escape, whereas when $z \leq -1$ the pair always escapes.

The results for the survival probability $S(p_T)$, with $\alpha = 1/2$ and $\beta = 1/4$, are shown in Figs. 3(a), 3(b), and 3(c) for the T_D values implied by eq. (5) (see Table 3) and for a decreasing sequence of radii: (a) $R = R_{\text{pb}} = 7.1$ fm, (b) $R = R_S = 3.8$ fm and (c) $R = 1$ fm, respectively. In all three cases, we observe that $S(p_T) \sim 0$, corresponding to essentially total suppression, at small p_T with our assumption of an equilibrated system. For $R = R_{\text{pb}}$ the system is large enough for the finite lifetime to be more important than its finite size. Therefore $S(p_T) = 1$ for $p_T \geq p_{T,\text{max}}$ while states with $p_T < p_{T,\text{max}}$ are suppressed. If the QGP is of smaller spatial extent, the survival probability can become unity for $p_T < p_{T,\text{max}}$ since a smaller p_T is sufficient for the pair to escape the system. This is illustrated by the results for $R = R_S$ and $R = 1$ fm displayed in (b) and (c) of Fig. 3. As R decreases, the largest p_T value for which suppression occurs decreases more rapidly for the Υ' and χ_b states than for the Υ because of their larger breakup time, t_D ; see Table 5. In fact, when $R = 1$ fm, $S(p_T) = 1$ for the Υ' at $p_T \approx 10$ GeV while the Υ remains suppressed up to $p_T \approx 20$ GeV, as shown in Fig. 3(c).

We should compare these results to other possible QGP scenarios.

- First, there is the possibility that we have overestimated the amount of screening that occurs for a given level of minijet production. As we have noted, see Table 5, the screening times, t_D , are generally shorter for the perturbative estimate of eq. (6) [even if quarks are not included by setting $n_f = 0$] than for the $SU(N)$ gauge parameterization given in eq. (5)⁸. The result is that there is no suppression of the Υ states for the 3-Flavor QGP in equilibrium if minijet initial conditions apply.
- It is also possible that the minijet density is different than we assumed in our calculations. For example, if the appropriate minijet momentum scale, p_0 , were larger (smaller) than the value of $p_0 = 2$ GeV assumed above, t_0 and, consequently, the minijet density, T_0 and, from eq. (16), t_D would all be smaller (larger). A lower minijet density could produce a different suppression pattern for the Υ family; *e.g.* a choice of p_0 is possible such that Υ production is not suppressed, while Υ' and χ_b production are.

⁸The ψ' and χ_c are an exception because the lower value of T_c found when quarks are included reduced the breakup temperature, resulting in a longer screening time.

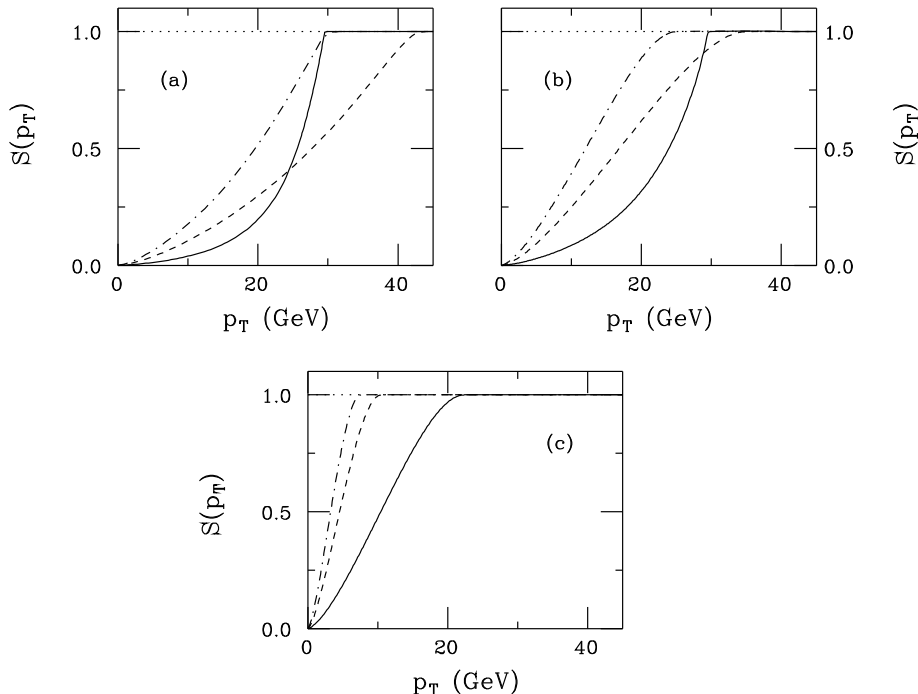


Figure 3: For the $SU(N)$ $\mu(T)$ of eq. (5) and the associated minijet initial conditions of $T_0 = 1.14$ GeV, $t_0 = 0.1$ fm, the suppression factor $S(p_T)$, calculated according to eq. (21), is shown for Υ (solid), Υ' (dashed), and χ_b (dot-dashed) production in three cases: (a) $R = R_{Pb}$; (b) $R = R_S$; and (c) $R = 1$ fm.

- We note that typical early estimates of the initial conditions without minijet production, $t_0 = 1$ fm and $T_0 = 250 - 300$ MeV at the LHC (see *e.g.* [12]), produce no bottomonium suppression regardless of the form of $\mu(T)$.
- An alternative set of initial conditions is obtained using the uncertainty principle [63, 64]. In this case, $t_0 \langle E \rangle \sim C \hbar c$, with $\langle E \rangle \sim 3T_0$ for a thermal average. In previous calculations, $C = 1$ and 3 were chosen. Those studies, using $T_c = 200$ MeV and assuming a 3-Flavor QGP, obtained $T_0 = 0.46$ GeV and $t_0 = 0.42$ fm for $C = 3$ and $T_0 = 0.81$ GeV and $t_0 = 0.08$ fm for $C = 1$ [64]. In Tables 5 and 6 we update these results for the pure gluon $SU(N)$ and 3-Flavor QGP cases, using the appropriate T_c for each. As can be seen from the formulae of Ref. [64], the 3-Flavor scenario has a higher T_0 than the $SU(N)$ case given our assumption that the final multiplicity is the same regardless of the initial conditions. We note that either choice of C produces

the same results because $T_0 \propto \sqrt{3/C}$ (as shown in [64]) and $t_0 T_0 \propto C/3$, implying that the C dependence cancels in the expression for t_D , eq. (16). Neither scenario leads to any bottomonium suppression, and suppression of the charmonium states is only possible for rather low p_T values.

- The final initial condition scenario that we discuss is based on a parton gas model as adopted for J/ψ suppression at RHIC and LHC energies in Ref. [65]. In this model one finds that the kinetic equilibration time is longer than for any of the cases discussed so far, $t_0 \sim 0.5 - 0.7$ fm. This time is reached when the momentum distributions are locally isotropic due to elastic scatterings and the expansion of the system. Chemical equilibrium is generally not assumed but the system moves toward equilibrium as a function of time. In this picture, the cooling of the plasma is more rapid than the simple Bjorken scaling picture [59] we have adopted, producing incomplete suppression at low p_T . To make a schematic comparison with our assumption of complete equilibrium, we give in Tables 5 and 6 the values of t_D and $p_{T,\max}$ for the onium states computed using the same T_0 and t_0 as employed in their calculation, derived from the HIJING Monte Carlo code [66]. (Note that we use the same initial values independent of the form assumed for $\mu(T)$.) Because the equilibration time of the parton gas is longer than that obtained from the minijet initial conditions, the time the system spends above the breakup temperature is also longer, leading to suppression for both the $SU(N)$ and the 3-Flavor forms of $\mu(T)$, even though T_0 is lower. These results are illustrated in Fig. 4 for the two $\mu(T)$ parameterizations. Figs. 4(a) and 4(b) illustrate the survival probability $S(p_T)$ for the $SU(N)$ plasma assuming $R = R_{\text{Pb}}$ and 1 fm, respectively. In the $SU(N)$ case, $p_{T,\max}$ is sufficiently large that the lead nucleus is already small enough for the p_T range of the suppression to be less than the calculated $p_{T,\max}$. The 3-Flavor QGP results are shown in Figs. 4(c) and 4(d) for $R = R_{\text{Pb}}$ and 1 fm, respectively. Here the temperature is not high enough for Υ suppression but the Υ' and χ_b are suppressed, albeit over a much smaller p_T range than in the $SU(N)$ case.

A given prediction for the survival probability $S(p_T)$ can be used to calculate the p_T distributions of the Υ states. Since $S(p_T)$ depends upon the T_D and τ_F of each Upsilon resonance, each state will have a unique p_T dependence, despite the fact that the p_T distributions determined from the color evaporation model are the same for directly produced Υ , Υ' and χ_b before inclusion of QGP effects. As we have noted, the precise $S(p_T)$ factors for the different Υ resonances also depend on the choice of $\mu(T)$, t_0 , T_0 , and R .

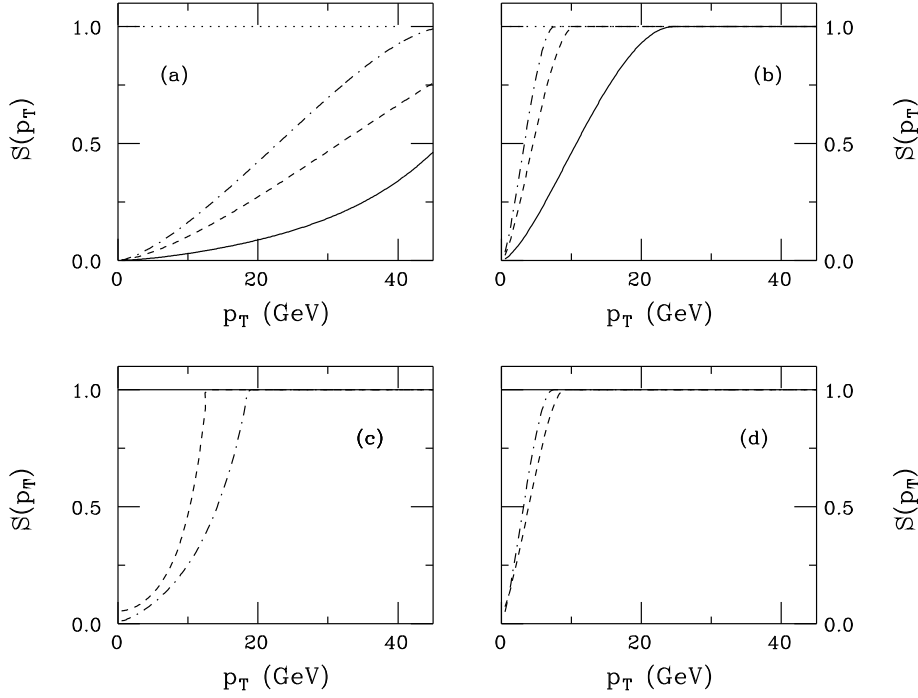


Figure 4: For parton gas initial conditions of $T_0 = 820$ MeV, $t_0 = 0.5$ fm, the suppression factor $S(p_T)$, calculated according to eq. (21), is shown for Υ (solid), Υ' (dashed), and χ_b (dot-dashed) production in four cases: (a) $R = R_{\text{Pb}}$ and $\mu(T)$ of eq. (5); (b) $R = 1$ fm and $\mu(T)$ of eq. (5); (c) $R = R_{\text{Pb}}$ and $\mu(T)$ of eq. (6); (d) $R = 1$ fm and $\mu(T)$ of eq. (6).

The resulting p_T spectra are shown in Fig. 5 in the case of $S(p_T)$ taken from Fig. 3(a), assuming the $SU(N)$ form of $\mu(T)$, with $R = R_{\text{Pb}}$, $t_0 = 0.1$ fm and $T_0 = 1.14$ GeV. The upper curves are the p_T distributions in pp collisions at $\sqrt{s} = 5.5$ TeV while the lower ones are the pp curves multiplied by $S(p_T)$ to indicate the p_T distribution expected in the presence of the quark-gluon plasma. Note that plasma production decreases the slope of the p_T distribution.

The raw p_T distributions before including the survival probabilities were obtained using the color evaporation model predictions calculated with the next-to-leading order $Q\bar{Q}$ code of Ref. [26]. It is well-known that at low p_T it is necessary to resum the next-to-leading $\ln(M^2/p_T^2)$ powers for each power of α_s to get an exponential factor. This has been extensively studied for W and Z production [67, 68, 69, 70, 71, 72]. The procedure involves computing a form factor in impact parameter (b) space, and then Fourier transforming back to p_T space. For $\Lambda_{\text{QCD}} \ll 1/b < M$, the form factor can be computed perturbatively; for $b \gtrsim 1/\Lambda_{\text{QCD}}$ non-perturbative

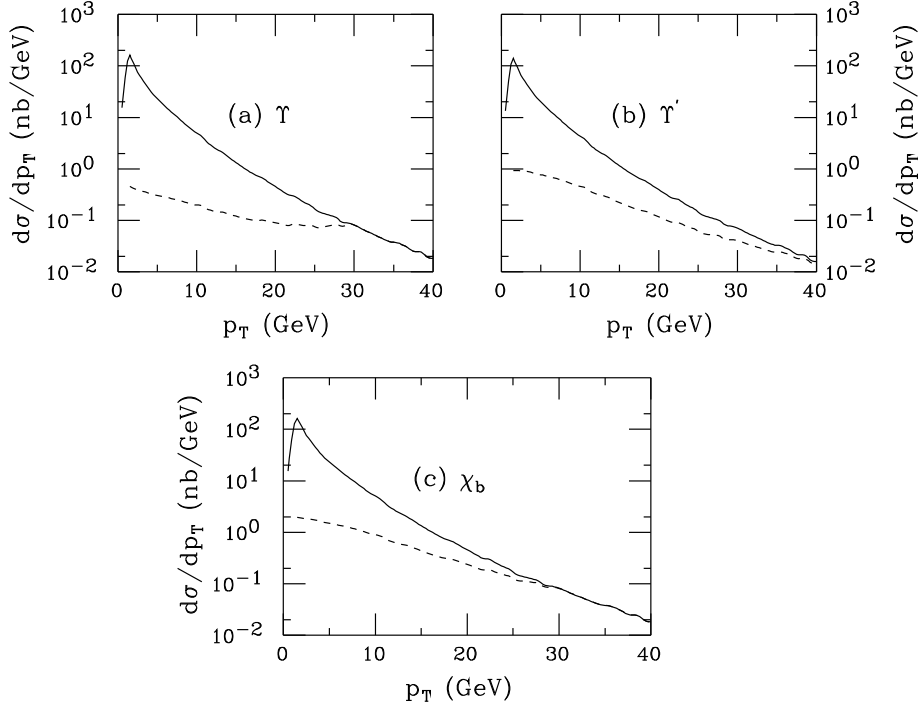


Figure 5: The p_T distributions for (a) Υ , (b) Υ' , and (c) χ_b production are given for pp interactions (solid) and plasma production (dashed). The plasma results are the pp distributions multiplied by $S(p_T)$ as computed for $R = R_{Pb}$, $t_0 = 0.1$ fm and $T_0 = 1.14$ GeV and assuming the SU(N) form of $\mu(T)$ as given in eq. (5); $S(p_T)$ for this case was plotted in Fig. 3(a). We have taken $\sqrt{s} = 5.5$ TeV. The differential cross sections (before including $S(p_T)$) are normalized to the integrated values tabulated in Table 4.

modeling is necessary. In the latter range, the conventional procedure is to introduce a cutoff in b and a non-perturbative factor in the b -space form factor. It is found [72] that the non-perturbative component dominates the p_T -dependence modifications for $p_T \lesssim 6$ GeV, implying substantial uncertainties for p_T -dependence in this domain. However, Ref. [72] also demonstrates that the ratio $[d\sigma(W)/dp_T]/[d\sigma(Z)/dp_T]$ is very insensitive to the non-perturbative uncertainties due to the fact that m_W is not very different from m_Z . Further, the ratio deviates only slightly from the perturbatively computed value. Applied to the closely-spaced resonances of the Upsilon family, the formalism of Ref. [72] implies that the color evaporation model predictions for the ratios of the production rates for different Υ states will also not be significantly modified by the non-perturbative physics. The ability to reliably compute a ratio such as Υ'/Υ as a function of p_T down to relatively

low p_T values is critical to the program described in the next section.

5 A program for determining the nature of the QGP

We have seen that the uncertainties in the initial conditions as reflected in t_0 and T_0 , the uncertainty in the QGP radius R , and the ambiguity in the temperature dependence of the screening mass, $\mu(T)$, all imply that there are many possible results for the relative suppression of the Υ states. The challenge will be to extract the correct plasma picture from the data. We describe below the inputs, procedures and detector features required in order that the production and suppression of the Υ states can be used as a tool to determine the true state of the plasma and the proper initial conditions. Data from the LHC and RHIC will prove complementary; it is likely that Upsilon family production rates must be measured at both machines in order to reach reliable conclusions. Further, measurements of the charmonium states at both LHC and RHIC will provide valuable information. We organize the following discussion into a series of (overlapping) tasks and requirements necessary to extract information about the QGP.

Checking the color evaporation model and establishing a baseline.

As a first step, the production rates and p_T spectra for the Υ states must be measured in pp collisions at the standard LHC nucleon-nucleon collision energy of 5.5 TeV and, by lowering the energy of the LHC still further, at 1.8 TeV.⁹ This will allow us to check the predictions¹⁰ of the color evaporation model. In particular, we must confirm that the the Υ'/Υ and Υ''/Υ ratios are *independent* of energy and p_T and that the (common) p_T -dependence of the individual cross sections agrees with the color evaporation prediction. These measurements will allow us to confirm our perturbative modeling and understanding of Υ production in the clean pp environment, thus establishing a baseline for comparison with results obtained for nuclear collisions.

Determining the effects of shadowing and nucleon absorption using RHIC data.

Next, we must determine if the Υ'/Υ ratio is independent of purely nuclear matter effects (*e.g.* shadowing and absorption) by measuring the ratio

⁹The lower energy measurement should agree with that obtained at the Tevatron [36] to the extent that valence quark distribution function contributions do not contribute significantly in $p\bar{p}$ collisions, but a direct pp measurement will remove the necessity of making this assumption in order to carry out the following program.

¹⁰Assuming that gluon fusion is dominant at both LHC and Tevatron energies.

in pA collisions. Since these studies are not possible at the LHC, this must be established at RHIC. The heaviest nuclear beam at RHIC will be gold, but the shadowing should be quite similar in gold and lead. Since RHIC is a dedicated heavy-ion facility, the PHENIX experiment at RHIC is expected to obtain several thousand Υ events per year along with a similar number of Υ' 's [73]. This should be sufficient to determine: a) the p_T dependence of the Υ'/Υ ratio in pA interactions where nuclear effects are present but no QGP is expected; and b) the magnitude of the Υ'/Υ ratio. If the ratio is the same (smaller) than in pp collisions, then shadowing (absorption) is probably the dominant purely nuclear effect. The dependence of the onium ratios on shadowing/absorption may also be established by studying ψ'/ψ in pA collisions: lower x partons are probed and the rates are higher.

If shadowing is dominant over absorption, then measurements of the actual magnitude of the gluon shadowing will be important if we are to use the absolute p_T -dependence of the onium cross sections instead of their ratios to analyze the QGP. It has been suggested that pA measurements of the dilepton continuum ($M \geq 1$ GeV) at RHIC will provide a measure of gluon shadowing since dileptons from charm production and decay (mainly from gluon fusion) will be the largest contribution in the mass region below the J/ψ [74]. Such charm studies are particularly useful because they probe gluon shadowing at the low x values that will be important for Upsilon production at the LHC. Measurements at RHIC for dilepton masses near the Υ mass probe parton x values of $x \sim 0.1$ (at $y \sim 0$), *i.e.* substantially above those appropriate at the LHC and also in a range where little shadowing is expected [75]. In order to probe small x values for dilepton masses near M_Υ , it would be necessary to accumulate good statistics for the Υ 's at high rapidity, which can be observed in the muon arms of the detector. An Υ with $y \sim +2$ or -2 will have $x_2 \sim 0.35$, *i.e.* in the EMC region, or $x_2 \sim 0.006$, in the shadowing region, respectively. The latter would probe nuclear effects on Υ production for gluon x values that are dominant for Υ production at the LHC around $y \sim 0$.

Perhaps the best way to determine the importance of nucleon absorption for the onium states is to measure the relative rapidities of the onium states and the initial nucleons since the baryon number in the central region of nuclear collisions at RHIC and LHC is expected to be small. If the nucleons and quarkonium states are far apart in phase space, the effects of nucleon absorption should be negligible. A zero-degree calorimeter or a forward hadron spectrometer, such as that of the BRAHMS detector at RHIC [76] could clarify this matter.

Determining the importance of comovers.

The use of onium production data for determining the nature of the QGP will be difficult if there are non-QGP mechanisms (other than simple shadow-

ing) affecting onium production that are comparable to the predicted QGP effects. We have already discussed one such mechanism, namely nuclear absorption. However, we concluded that it was relatively benign since it should have little p_T dependence and will not be important if the projectile and target fragmentation regions are well separated from the quarkonium states in the central region. A second mechanism of concern is the breakup/absorption of the onium states through interactions with comoving secondary hadrons. Indeed, the observed J/ψ suppression [15, 16] at $\sqrt{s} = 17$ GeV has been attributed to interactions with these comovers [20]. The comovers should also be present at higher energies. Such hadronic scattering can affect both the ψ states and the Υ states. For example, the comovers can easily break up the J/ψ if the combined comover+ J/ψ center-of-mass energy is above the $D\bar{D}$ threshold. Since the separation between the onium mass and the threshold is smaller for the higher onium states, the higher states will be more easily broken apart by comovers. Thus, comovers could cause ratios such as Υ'/Υ and ψ'/ψ to be smaller than expected. The Υ , being the most tightly bound of the onium states, should be least affected. Note that this is precisely the same as expected from nucleon absorption, which should be largest for states with large radii and small mass thresholds. As discussed earlier, if the comovers are mesons, the onium-comover absorption cross section should be $\sim 2/3$ the onium-nucleon absorption cross section.

Although the interpretation of J/ψ suppression at $\sqrt{s} = 17$ GeV as being due to comover scattering implies high hadronic densities in the present experiments, a hadronic interpretation of quarkonium dissociation would be much less plausible at LHC energies, where, for all cases considered in Table 5, T_0 is significantly above T_c . The reasoning is as follows. For such high initial temperatures, it is almost certain that a QGP will form, delaying the creation of hadrons until the $Q\bar{Q}$ pair or onium state has passed through much of the material. Thus, there would be little opportunity for interactions with comovers until the late stages of the collision. The T_0 values for RHIC (Table 6) are also generally higher than T_c and significant breakup due to interactions with comovers again seems unlikely if a QGP is formed.

While the above argument suggests that comover absorption will not significantly impact onium production, it will be important to try to determine the importance of comovers directly from experiment. We outline several possible approaches.

- In pA collisions a QGP is not formed. Thus, as noted earlier, in pA collisions the dilepton spectrum in the $M > 1$ GeV region, being primarily due to $c\bar{c}$ production and decay, should provide a reliable probe of shadowing. Comovers will have only a small influence on open charm mesons because the scattering is elastic — a πD interaction will change the momentum distribution of the D but will not take the charm out

of the system. Nucleon- D scattering is also expected to be elastic. On the other hand, a J/ψ -comover interaction is likely to break up the J/ψ into $D\bar{D}$ pairs. By comparing the ‘shadowing’ on and off the resonance, we can obtain a firmer handle on the magnitude of comover absorption of the J/ψ .

- In nucleus-nucleus collisions, the density of comovers which can absorb the onium state would be larger still, with the largest density in central collisions. Since these densities are related to the final multiplicity and thus to the transverse energy of the collision, perhaps one of the best ways to check the importance of comover breakup and absorption is to trigger on peripheral collisions (for which a QGP is not formed). One would compare predictions for the ψ and Υ states based on shadowing in peripheral collisions with actual measurements to see if there is extra suppression due to comover breakup or absorption. Such collisions could provide very valuable guidance on whether comover absorption is important. In addition, one could compare (as above) the dilepton spectrum on and off the ψ resonance.

Comover absorption will also not occur if the onium p_T is large enough. Calculations of comover suppression as a function of p_T appear in Refs. [77, 78, 79]. The range of p_T over which comover suppression occurs should not depend strongly on energy. One can make a crude estimate of the p_T range of comover interactions as in eq. (17). In this case,

$$p_{T,\max}^{\text{co}} = M\sqrt{(t_{\text{co}}/\tau_{\text{co}})^2 - 1}, \quad (24)$$

where t_{co} depends on the size of the system, $t_{\text{co}} \sim R/v_{\text{rel}}$, (v_{rel} is the relative velocity of the onium and the comovers, 0.6 for ψ -comover interactions at the CERN SPS) and $\tau_{\text{co}} \sim 2$ fm is the comover formation time in a nucleus-nucleus collision. Since we assume comovers are final-state hadrons, there is no T_0 dependence and since the p_T range depends on the comover formation time rather than the onium formation time, $p_{T,\max}^{\text{co}}$ changes by 20% or less for each onium family. When $R = R_{\text{Pb}}$, $p_{T,\max}^{\text{co}} = 5.8M$. Note that if a QGP is formed, τ_{co} could be even longer since the comovers would not form until after the QGP hadronizes. At the very least, the above comparisons should allow us to determine the maximum p_T up to which comover absorption is important.

The influence of comover absorption is clearly an important issue. In the following discussion, we assume that all nuclear and comovers effects on the onium production cross sections can be unfolded or proven to be small.

Using RHIC data to establish the general nature of the QGP.

At RHIC ratios such as Υ'/Υ and ψ'/ψ will be measured in nucleus-nucleus collisions. For minijet initial conditions or initial conditions based on the uncertainty relations, the short initial time scales result in the prediction that there should be no significant suppression at RHIC for any of the onium states, regardless of the form of $\mu(T)$. However, in the parton gas model the long t_0 implies that suppression of the Υ states is possible for the $SU(N)$ (but not the 3-Flavor) form of $\mu(T)$. Further, the ψ states are predicted to be suppressed for both the $SU(N)$ and 3-Flavor forms of $\mu(T)$. Thus, the suppression pattern of the ψ and Υ states will help distinguish the $\mu(T)$ dependence if significant suppression is observed. Specifically:

- If all the ratios are independent of p_T , then either no plasma has been produced or the initial conditions of the plasma are unfavorable for suppression to occur.
- If the ψ'/ψ ratio depends on p_T , but the Υ'/Υ ratio does not, the most consistent picture is that a QGP has formed with initial conditions like those of the parton gas model and $\mu(T)$ is of the 3-Flavor form given in eq. (6).
- If both ratios are p_T -dependent, then parton-gas-like initial conditions are required and the screening mass is more likely to be of the $SU(N)$ form as in eq. (5).

Analyzing the QGP at the LHC.

One advantage of the LHC over RHIC is that onium suppression can occur for a much broader range of possible initial conditions. In particular, at the LHC the minijet initial conditions produce an initial temperature T_0 that is sufficiently large that the fast equilibration predicted (*i.e.* small t_0) does not prevent suppression. More generally, the higher T_0 possible at the LHC will be crucial since fast equilibration is perhaps more plausible.

The question we now address is how to best determine t_0 and other features of the QGP. A high statistics study of the Υ'/Υ ratio as a function of p_T may prove conclusive. If significant p_T -dependence of Υ'/Υ is found for $p_T \gtrsim 10$ GeV in Pb+Pb collisions at 5.5 TeV, then it will be virtually certain that a quark gluon plasma was formed. (As argued at the end of the previous section, any p_T -dependence of this type of ratio arising from low- p_T perturbative or non-perturbative resummation effects should be small, and effects from comovers/absorption/shadowing should be absent once p_T is reasonably large.) The precise behavior of the Υ'/Υ ratio can then be used to strongly constrain the QGP model parameters. In particular, the ratio will be very different if only the Υ' is suppressed in comparison to the case where both states are suppressed.

Prompt Production Ratios

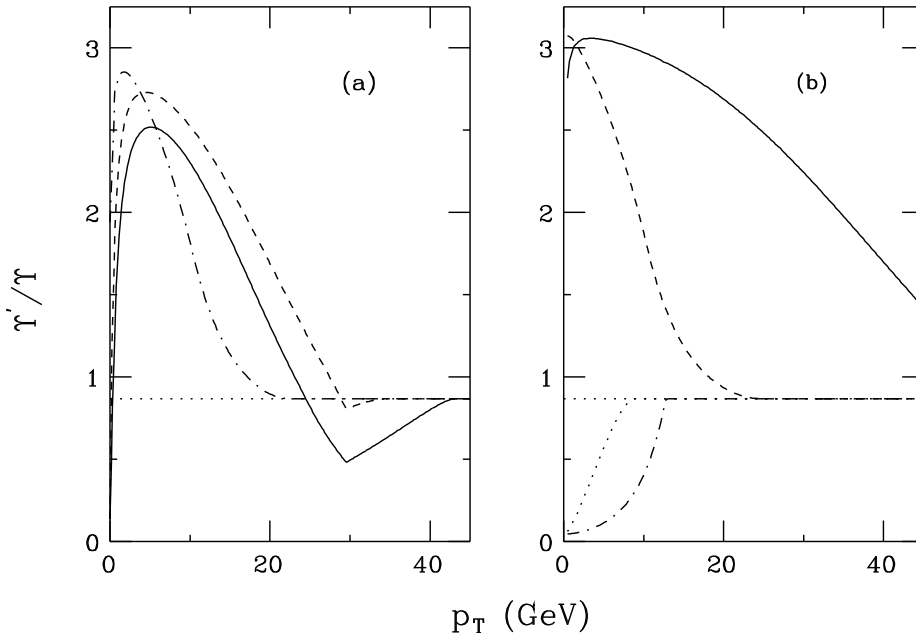


Figure 6: The direct or prompt Υ'/Υ ratio as a function of p_T is shown for several choices of initial conditions at the LHC. In (a), we show results for the minijet model with the $SU(N)$ form of $\mu(T)$, eq. (5), (for which $T_0 = 1.14$ GeV and $t_0 = 0.1$ fm) taking $R = R_{Pb}$ (solid), $R = R_S$ (dashed), $R = 1$ fm (dot-dashed). In (b), we consider the parton gas model with $T_0 = 0.82$ GeV and $t_0 = 0.5$ fm, and show results for the $SU(N)$ $\mu(T)$ with $R = R_{Pb}$ (solid) and $R = 1$ fm and for the 3-Flavor $\mu(T)$ from eq. (6) with $R = R_{Pb}$ (dot-dashed) and $R = 1$ fm (dotted).

In Fig. 6, we show the Υ'/Υ ratio for several sets of initial conditions. The ‘prompt’ ratio displayed is that obtained if only directly produced Υ' and Υ states are included. In other words, the ratio is computed using $f_{\Upsilon'}^d$ and f_{Υ}^d from eq. (13). We will return shortly to the issue of whether or not this prompt ratio can be experimentally measured.

Fig. 6(a) displays results obtained when the minijet initial conditions are used with $t_0 = 0.1$ fm and $\mu(T)$ is as given in eq. (5). Both the Υ and Υ' states are suppressed and the solid, dashed and dot-dashed curves (for $R = R_{Pb}$, R_S and 1 fm, respectively) show that the p_T -dependence of the ratio can distinguish different plasma radii. At low p_T the Υ is actually more suppressed than the Υ' , leading to a significantly larger ratio than that expected in low energy pp collisions (or found in current $p\bar{p}$ measurements). For a large R , the ratio eventually drops below the value expected in the

absence of QGP effects (*i.e.* for large enough p_T). The point at which this shift occurs is at $p_T \approx 25$ GeV if $R = R_{\text{Pb}}$ and at ≈ 29 GeV for $R = R_S$. The kink in these ratios at 30 GeV occurs at the point where the Υ is no longer suppressed. In a system with a smaller $R = 1$ fm radius, the Υ is always more suppressed than the Υ' so that the ratio returns to the pp value at $p_T \approx 20$ GeV.

Fig. 6(b) shows the ratio computed using the parton gas initial conditions. When the $SU(N)$ $\mu(T)$ is assumed, the behavior is similar to the minijet case although when $R = R_{\text{Pb}}$ the increase in Υ'/Υ persists to much larger p_T . When $R = 1$ fm, the result is almost indistinguishable from the minijet case with the same radius. The maximum of the ratio is $\sim 10\%$ larger at $p_T \sim 1-2$ GeV, but this may be difficult to distinguish. If the 3-Flavor [eq. (6)] scenario is assumed for the screening mass, then the Υ' is suppressed while the Υ is not and the p_T -dependence of the ratio is quite different. The dot-dashed and dotted curves of Fig. 6(b) show that until the effects of the plasma disappear, the ratio is less than expected in the absence of QGP formation. However, it is more difficult to differentiate between a system the size of the lead nucleus or a system with $R = 1$ fm unless the measurement is made with high statistics. We have already noted that if significant suppression is observed at RHIC in the ψ'/ψ ratio as a function of p_T and Υ suppression is observed at RHIC, the general behavior of $\mu(T)$ should be relatively clear by the time the LHC measurement is made.

Finally, we recall that for the uncertainty relation initial conditions, both t_0 and T_0 are small even at the LHC and no suppression is expected for the Upsilon states. To learn about the existence and nature of a QGP via measurements of onium production will not be possible for such models.

The importance of separating prompt from indirectly produced onium states.

An important issue is whether or not the ‘prompt’ ratio discussed above can be extracted experimentally. We saw earlier that a significant fraction of Υ production arises from Υ' and χ_b (χ_b denotes the collective $\chi_{bi}(1P, 2P)$, $i = 0, 1, 2$ states) production followed by $\Upsilon' \rightarrow \Upsilon X$ and $\chi_b \rightarrow \gamma \Upsilon$, respectively. Further, some of the Υ' 's come from $\chi_{bi}(2P) \rightarrow \gamma \Upsilon'$. We can only isolate the prompt ratio discussed above if we can veto such decay sources of the Υ and Υ' . In the case of the χ_b decays, this will only be possible by detecting the associated photon and reconstructing the χ_b . The ability of the LHC detectors to do this will be limited at low p_T for two reasons: i) there is a large π^0 background from which it is difficult to extract isolated γ 's until the p_T of the γ becomes substantial ($\gtrsim 10$ GeV) and ii) the photon energy resolution will be poor at low p_T . In order to veto $\Upsilon' \rightarrow \Upsilon X$ decays we must be able to detect the $X = \pi^+\pi^-, \pi^0\pi^0$ decay products. This latter may be impossible; however, this indirect decay is only responsible for about 13% of

Production Ratios With Indirect Decays

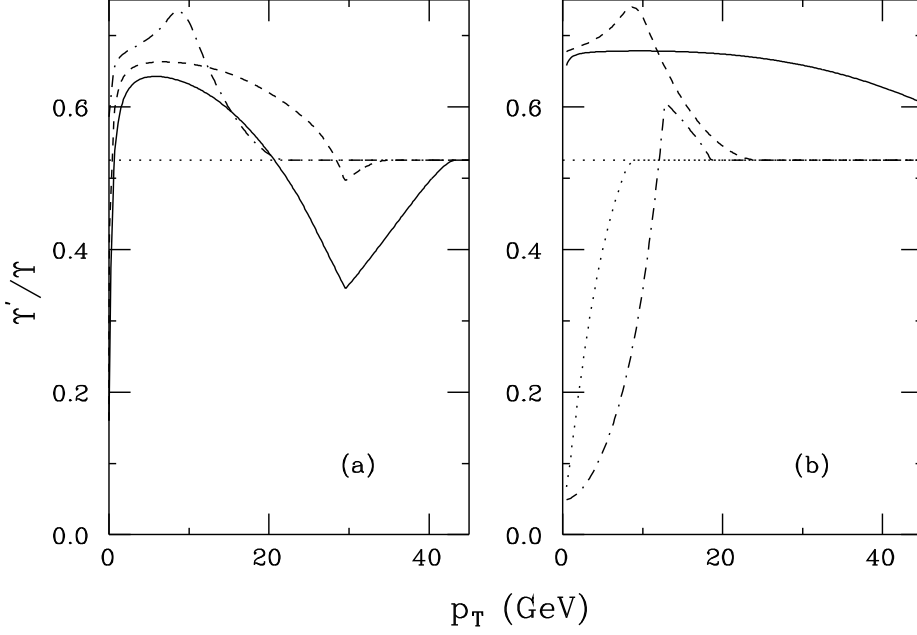


Figure 7: The Υ'/Υ ratio including indirect decays as a function of p_T is shown for several choices of initial conditions at the LHC. In (a), we show results for the minijet model with the $SU(N)$ form of $\mu(T)$, eq. (5), (for which $T_0 = 1.14$ GeV and $t_0 = 0.1$ fm) taking $R = R_{Pb}$ (solid), $R = R_S$ (dashed), $R = 1$ fm (dot-dashed). In (b), we consider the parton gas model with $T_0 = 0.82$ GeV and $t_0 = 0.5$ fm, and show results for the $SU(N)$ $\mu(T)$ with $R = R_{Pb}$ (solid) and $R = 1$ fm and for the 3-Flavor $\mu(T)$ from eq. (6) with $R = R_{Pb}$ (dot-dashed) and $R = 1$ fm (dotted).

the Υ' 's, so that if the χ_b decays can be vetoed we will obtain a result much like the prompt ratio plotted in Fig. 6. If the χ_b decays cannot be vetoed, then we must consider all sources of the Υ' and Υ , each of which will be associated with a different suppression factor. Numerically, it is sufficient to consider:

$$\frac{\Upsilon' + \chi_b(2P)(\rightarrow \Upsilon') + \Upsilon''(\rightarrow \Upsilon')}{\Upsilon + \chi_b(1P, 2P)(\rightarrow \Upsilon) + \Upsilon'(\rightarrow \Upsilon) + \Upsilon''(\rightarrow \Upsilon)}. \quad (25)$$

In computing this ‘indirect’ Υ'/Υ ratio we have assumed that the survival probability, $S(p_T)$, of the $\chi_b(2P)$ states is the same as that for the $\chi_b(1P)$ states and that $S(p_T)$ for the Υ'' is the same as for the Υ' .

The indirect ratio, defined in eq. (25) is plotted in Fig. 7. Clearly, the indirect ratio is somewhat less sensitive to changes in R and $\mu(T)$ than is the direct Υ'/Υ ratio. If the $SU(N)$ form of $\mu(T)$ is appropriate, the figure indi-

cates that a measurement at the 20% level is needed to distinguish between the pp value of the ratio and the QGP prediction including indirect decays in both the minijet and parton gas initial condition scenarios. (If there are substantial systematic errors in the ratio, the detection of a deviation might be most difficult for the parton gas $SU(N)$ case when $R = R_{\text{Pb}}$, since in this case the ratio varies slowly with p_T .) If the slowly-growing 3-Flavor form of $\mu(T)$ is correct, the dot-dash and dotted curves of Fig. 7(b) show that the parton gas model predicts significant and strongly p_T -dependent departures from the Υ'/Υ ratio expected in the absence of a QGP. It would even be possible to determine the size of the system using the indirect ratio — as shown in Fig. 7(b) the χ_b contribution to the Υ causes the Υ'/Υ ratio to increase above the pp level at $p_T \approx 12$ GeV for $R = R_{\text{Pb}}$ but not for $R = 1$ fm.

Thus, all is not lost if only the indirect ratio can be measured, but sensitivity is reduced and the accuracy with which the Υ'/Υ ratio can be measured becomes crucial. Also, our ability to predict theoretically or measure in other contexts with some reliability the relative values of the f^d 's becomes quite important.

Estimates of the statistics required and the importance of vetoing indirect decays.

The ability to employ the Υ'/Υ ratio to analyze the nature of the QGP will depend crucially on the statistics available. For $\sigma_{NN}T_{\text{PbPb}}(\mathbf{0})L_{\text{int}}^{\text{PbPb}} = 4.973 \times 10^3 \text{ nb}^{-1}$ per month, as assumed in Table 4, and the $d\sigma(pp)/dp_T \times S(p_T)$ spectra of Fig. 5, which range very roughly from 1 nb/GeV to 0.1 nb/GeV over the p_T range of interest, we find $\sim 5 \times 10^3$ falling to $\sim 5 \times 10^2$ events per GeV for the individual Υ , Υ' and χ_b resonances. For branching ratios of $B_{\Upsilon} = 0.025$ and $B_{\Upsilon'} = 0.013$ and an efficiency/acceptance factor of 33% (which, as noted earlier, applies to the CMS detector), this leaves us with ~ 41.3 (~ 21.5) falling to ~ 4.13 (~ 2.15) Υ (Υ') events per GeV per month of running. For a 2 GeV bin size, 12 months of running and negligible background (see below), we obtain Υ (Υ') statistical accuracies of $\sim 3\%$ ($\sim 4.5\%$) at low p_T rising to $\sim 10\%$ ($\sim 14\%$) at $p_T \sim 25 - 30$ for the individual spectra, and of 5.4% rising to 17% for the Υ'/Υ ratio. Thus, if the prompt ratio can be extracted, somewhat more than a year of running at $L_{\text{int}}^{\text{PbPb}} = 2.59 \text{ nb}^{-1}$ per month would be sufficient to measure the ratios with the required accuracy over the full range of p_T values of interest. If the Υ'/Υ ratio can only be measured including indirect decays, greater accuracy is required at large p_T . Roughly 36 months of running at $L_{\text{int}}^{\text{PbPb}} = 2.59 \text{ nb}^{-1}$ per month would be required to achieve $\lesssim 10\%$ accuracy for the ratio at $p_T \sim 30$ GeV. Since this amount of running in the heavy ion mode at the LHC is quite unlikely, we see how important the vetoing of indirect decays is if we are to use the Υ'/Υ ratio to analyze the QGP.

The importance of mass resolution.

Also crucial to the program is the ability to resolve the Υ , Υ' and Υ'' resonances from one another. The CMS detector provides excellent mass resolution in the $\mu^+\mu^-$ mode, of order 40 MeV, adequate for clean separation of the Υ , Υ' and Υ'' signals (see Fig. 12.31b in Ref. [21]). As also shown in [21], the excellent resolution implies a very modest level of background under the Υ peaks. Preliminary estimates of the mass resolution for the ATLAS detector are less encouraging, of order 200 – 300 MeV [80], for which separation of the resonances would not be possible.

Other onium ratios.

In the above discussion, we have focused on the Υ'/Υ ratio. Other ratios would provide complementary information. However, the Υ''/Υ ratio is a factor of 4 smaller [see eq. (13)] at the direct, *i.e.* prompt, level and statistics would be a problem. The direct/prompt $\chi_b(1P)/\Upsilon$ ratio is similar to the Υ'/Υ ratio, the major difference being that the $\chi_b(1P)/\Upsilon$ ratio never decreases below the pp level at high p_T in the $SU(N)$ case since $p_{T,\max}^{\chi_b} \approx p_{T,\max}^{\Upsilon}$ (see Figs. 3 and 4). Further, if the $\chi_b(1P)$ radiative decays can be detected with reasonable efficiency, the statistical accuracy with which the $\chi_b(1P)/\Upsilon$ ratio can be measured would be comparable to that for the Υ'/Υ ratio, thus making it a most valuable addition. This adds to the importance of being able to trigger efficiently on the decay photons so as to isolate these two direct ratios.

Extracting individual survival probabilities and using Z production to control systematics.

So far, we have considered only ratios of onium rates. However, it will be important to know that suppression of the general type expected is taking place in the individual spectra contributing to these ratios. It would be even more valuable if a quantitative determination of $S(p_T)$ for the different resonances were possible through a direct comparison of the differences between the pp spectra and the Pb+Pb spectra at 5.5 TeV, as illustrated in Fig. 5. In principle, the ratio of the properly normalized Pb+Pb spectrum to the pp spectrum for a given resonance simply gives $S(p_T)$,¹¹ *provided* there are no non-QGP effects that can also alter the Pb+Pb spectrum. However, it is very likely that there will be some nuclear effects from shadowing, comovers and absorption. Effects from comovers and absorption cannot be disentangled except as described earlier. However, there is some possibility of obtaining additional information regarding shadowing.

The strength of shadowing depends upon the x values at which the parton distributions are probed. Thus, the RHIC pA measurements of onia produc-

¹¹As argued in the previous section, non-perturbative resummation effects upon the p_T distributions will cancel out in such a ratio.

tion, while helpful, cannot directly determine the full effect of shadowing at 5.5 TeV where we wish to determine the presence of the QGP and measure $S(p_T)$. An independent test of the shadowing effect using measurements at $\sqrt{s} = 5.5$ TeV would be of great value for checking our understanding of shadowing and assessing the accuracy with which it can be unfolded from the data so as to reveal the QGP effects directly.

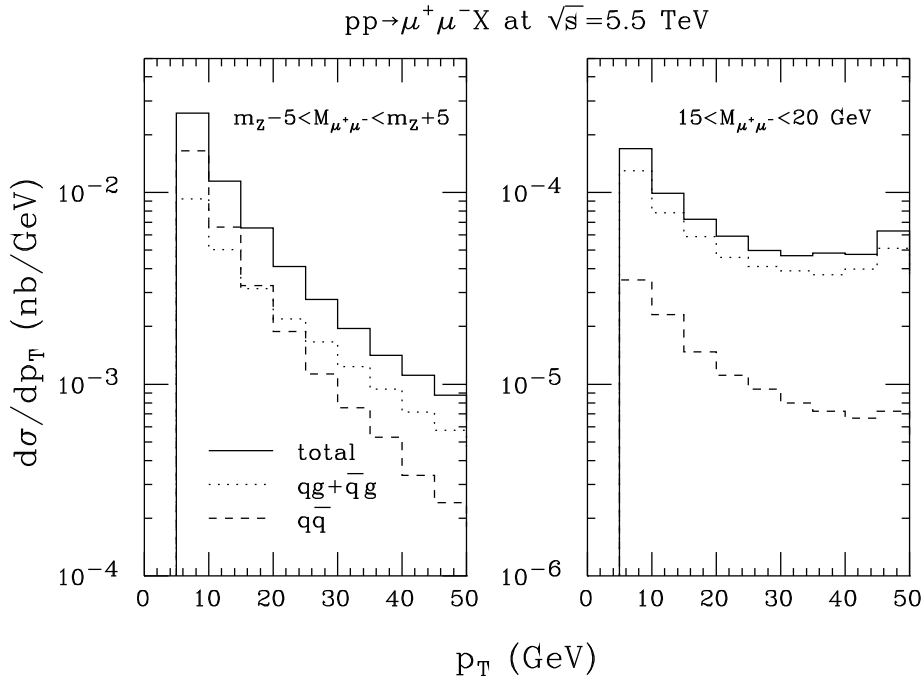


Figure 8: In (a), we plot $d\sigma/dp_T$ for $pp \rightarrow \mu^+\mu^- X$ at $\sqrt{s} = 5.5$ TeV as a function of p_T for Z production (defined by $m_Z - 5 \text{ GeV} \leq M_{\mu^+\mu^-} \leq m_Z + 5 \text{ GeV}$). In (b), the same cross section is plotted for $15 \text{ GeV} \leq M_{\mu^+\mu^-} \leq 20 \text{ GeV}$. The separate contributions from $q\bar{q}$ and $qg + \bar{q}g$ collisions are indicated by dashed and dotted histograms, respectively.

In the current experiments at the CERN SPS, J/ψ production is compared to the dilepton continuum [15, 16]. The continuum is assumed to be produced via the Drell-Yan (γ^* , Z^* -exchange) process and is, in fact, Drell-Yan-like in its behavior. At RHIC energies and higher, the continuum will be more difficult to understand because of the important contribution from semileptonic $c\bar{c}$ and $b\bar{b}$ decays. Not only are there uncertainties in the total $c\bar{c}$ cross section, but the heavy quark decays are also subject to nuclear effects. The relatively small Drell-Yan contribution is also subject to shadowing effects in the mass range between the J/ψ and the Υ . Another choice is needed. One possibility is Z production. Because the Z is produced in

point-like fashion, the difference between the p_T -dependence of the Z in pp collisions vs. Pb+Pb collisions will not be influenced by the quark-gluon plasma¹².

Figure 8 illustrates the cross section for Z production as a function of p_T at $\sqrt{s} = 5.5$ TeV assuming no shadowing. There, we plot $d\sigma/dp_T$ for $pp \rightarrow ZX$ and the separate contributions from $q\bar{q}$ and $qg + \bar{q}g$ collisions. (The distributions include 1-loop corrections to the $Z + jet$ cross section¹³, but do not include low- p_T resummation effects.) To obtain the number of events per month per GeV coming from central collisions¹⁴, we multiply by the factor $\sigma_{NN}T_{PbPb}(\mathbf{0})L_{\text{int}}^{\text{PbPb}} = 4.973 \times 10^3 \text{ nb}^{-1}$. At $p_T = 50$ GeV, the cross section is of order 10^{-3} nb/GeV , implying about 2 events per GeV for 40% acceptance and detection efficiency. Thus, for a 5 GeV bin we obtain about 10 events in this bin per month of running. After a year of running, this would yield a statistical accuracy of order 9%. At low p_T , event rates are a factor of $\gtrsim 10$ larger, yielding correspondingly greater accuracy. The predicted effects of the QGP, see for example Figs. 3 and 4, typically imply survival probabilities that differ by much larger percentages compared to unity. In any case, as estimated earlier, the errors in the measurements of the Upsilon resonance spectra will be larger. Thus, production rates in the $p_T \lesssim 50$ GeV domain are high enough that $Z \rightarrow e^+e^-, \mu^+\mu^-$ can provide a standard of comparison. Of course, we will also wish to measure Z production in pp collisions at $\sqrt{s} = 5.5$ TeV so as to determine if shadowing and other nuclear effects have impacted the Pb+Pb spectra. Good statistical accuracy for up to $p_T = 50$ GeV requires integrated luminosity for pp collisions of order $L = 0.01 \text{ fb}^{-1}$, which should be easily achieved, even at this reduced energy, by running for a few weeks.¹⁵

The two difficulties with using Z production as a benchmark are: (i) m_Z is much larger than the masses of the Upsilon resonances and (ii) the $q\bar{q}$ and $qg + \bar{q}g$ parton luminosities are probed vs. the gg luminosities responsible for $b\bar{b}$ production.

- The large size of m_Z compared to the Upsilon family masses reduces the value of Z production as a benchmark for two reasons. First, shadowing and related nuclear effects may well be dependent upon Q^2 . For

¹²Once again, this ratio will be very insensitive to low- p_T perturbative and non-perturbative resummation modeling.

¹³We thank U. Baur for providing a program against which to check our own calculations.

¹⁴We wish to restrict observations to central collisions in case shadowing and nuclear effects (that might possibly be present for the Z) for peripheral collisions are somewhat different.

¹⁵If we assume that low-luminosity running yields pp integrated luminosity of 10 fb^{-1} per year at $\sqrt{s} = 14$ TeV and that instantaneous luminosity falls as E^2 , then the corresponding integrated luminosity at $\sqrt{s} = 5.5$ TeV would be $\sim 1.5 \text{ fb}^{-1}$ per year or $\sim 0.03 \text{ fb}^{-1}$ per week.

example, in the limit of large Q^2 , holding the parton x fixed, shadowing becomes stronger in some models (see, *e.g.*, Ref. [81] whereas in others it is predicted to disappear altogether (see, *e.g.*, Ref. [82]). See also Ref. [83]. Thus, it is very possible that the shadowing at $Q^2 = M_Z^2$ will differ substantially from that at $Q^2 = m_Z^2$. Second, the x values probed ($x \sim m_Z/\sqrt{s} \sim 0.016$ at $y = 0$) are much larger than in Upsilon production at the same energy. (Detailed measurements as a function of the Z rapidity would provide information about smaller x values, but require more luminosity for good statistics.)

- The separate contributions of the $q\bar{q}$ vs. $qg + \bar{q}g$ densities to the Z spectrum appear in Fig. 8. We observe that $q\bar{q}$ collisions are dominant for $p_T \lesssim 15$ GeV; for higher p_T values $qg + \bar{q}g$ collisions dominate. Thus, to probe nuclear effects on the g distribution at $Q^2 = m_Z^2$, we must have knowledge of their effects on the q and \bar{q} distributions for x values in the vicinity of those being probed at this same Q^2 . At low to moderate Q^2 the nuclear effects on q and \bar{q} PDFs are rather well measured and do not appear to be strongly Q^2 dependent [57]. However, there is currently no direct measurement of q and \bar{q} shadowing at small x with Q^2 values as high as m_Z^2 . If nuclear beams become available at HERA, then direct measurement of shadowing at appropriate x and Q^2 values would be possible.

Even though Z production does not directly probe gluon shadowing at the x and Q^2 values of interest for Upsilon production, Z production would be of considerable value in developing a reasonable theoretical understanding or model of shadowing. If we measure the p_T dependence of Z production and find that it is consistent with one or more theoretically reasonable models of shadowing, this will already be a very important benchmark in that we can be confident there is not some totally unexpected physics occurring in nucleon-nucleon collisions. Of course, it is vital that Z production be measured both in Pb+Pb and in pp collisions at $\sqrt{s} = 5.5$ TeV in order for us to develop confidence that we understand the impact of shadowing and other purely nuclear effects.

Given the above issues regarding Z production, it would be advantageous if we could measure lepton pair production at pair masses nearer to those of the Upsilon states so as to constrain shadowing and nuclear effects at parton x and Q^2 values closer to those of direct relevance. We have already noted that we expect a large background from $c\bar{c}$ and $b\bar{b}$ production processes for lepton pair masses lower than the Upsilon family masses. At these low masses, this background will be very difficult to veto by requiring that the leptons be isolated because of the high density of soft tracks in the Pb+Pb collision environment. In the mass region above about 15 GeV the dilepton rate from

$c\bar{c}$ ($b\bar{b}$) pair production is predicted to be smaller than (comparable to) that from γ^* , Z^* -exchange [84]. Further, in this higher mass range, vetoing the $b\bar{b}$ component using isolation requirements on the leptons might prove feasible at a level adequate to extract the pure DY dilepton spectrum. In Fig. 8, we have plotted $d\sigma/dp_T$ for production of muon pairs with $15 \text{ GeV} \leq M_{\mu^+\mu^-} \leq 20 \text{ GeV}$ coming from γ^* , Z^* -exchange. We note that in this case the $qg + \bar{q}g$ collision component is always dominant, as would be desirable for learning as much about gluon shadowing as possible. However, the cross section is nearly a factor of 100 below that for production at the Z resonance, implying that statistics would be a factor of 10 worse. Even a year of running will not provide enough Pb+Pb luminosity to yield measurements that are sufficiently accurate to constrain the shadowing and nuclear effects at the needed level ($\lesssim 5 - 10\%$). Thus, the low rate and uncertainty regarding our ability to veto the $b\bar{b}$ background imply that we should not count on being able to use dilepton pairs below the Z mass region to improve our understanding of nuclear effects on the gluon PDFs. Nonetheless, the possibility of doing so should not be ignored and appropriate data, including event characteristics that might allow vetoing, should be collected.

HERA measurements of the nuclear g , q , and \bar{q} densities as a function of x and Q^2 would greatly assist in a reliable extraction of $S(p_T)$. Measurements overlapping the regions of interest for Υ and Z production at 5.5 TeV would be possible for an appropriate design of the facility. Using the HERA measurements for $x \sim 0.02$ and $Q^2 = m_Z^2$, it would be possible to unfold the shadowing effects in Z production and verify that the underlying p_T spectrum is that expected on the basis of the Drell-Yan mechanism. This would allow a high degree of confidence that we could use the HERA measurements at the x and Q^2 values appropriate to onium production to unfold the underlying p_T spectra of the onia as influenced only by absorption, comovers, and the quark-gluon plasma, with the latter hopefully having a much larger impact.

6 Discussion and conclusions

We have found that expectations for Υ (and also ψ) resonance production in Pb+Pb collisions at the LHC are very dependent upon the nature and details of the quark-gluon plasma. We have demonstrated that, far from being an impediment to our extracting the QGP physics, this dependence may very well allow us to determine much about the fundamental nature of the QGP, including: the energy density, the initial temperature, the plasma radius, and the temperature-dependent screening mass. Although we have kept the discussion of quarkonium production and suppression as general as possible, we chose the Υ family to examine in detail. The Υ rate is high

enough for statistically significant measurements to be made, particularly at the LHC. The Υ is also less affected by interactions with hadronic matter, providing a less ambiguous signal than the charmonium states. Strikingly different expectations for the p_T -dependence of the Υ'/Υ ratio, the example upon which we focused, are found depending upon whether or not the QGP is formed and on the QGP properties. While our calculations of the survival probability are rather schematic, *e.g.* assuming full equilibration, they reflect the correct general trend for the scenarios discussed.

The much higher energy of the LHC could be crucial for QGP suppression of onium production to be possible. This would be the case, for example, in the minijet model of the initial conditions. The high minijet density at the LHC implies that the p_T spectra of the Υ resonances in this model are likely to be highly sensitive to details of QGP formation. In contrast, at RHIC, the minijet density will be a factor of 10 to 30 smaller, and the maximum initial temperature predicted is $T_0 \sim 0.5$ GeV. Thus no suppression is expected. Initial conditions such as those predicted in parton gas models, for which the QGP takes longer to equilibrate, predict still stronger suppression at the LHC and could also lead to some suppression being observed at RHIC, depending upon the temperature dependence of the screening mass in the $b\bar{b}$ potential. There are also models of the initial conditions that predict no suppression even at the LHC. We point out that even a very high T_0 does not guarantee plasma suppression. Models assuming a slow equilibration result in greater suppression because of the longer time the system spends in the screening region with $T > T_D$.

Even if suppression is not present at RHIC, it is only at RHIC that pA measurements will be possible. Despite the lower energy, these pA measurements will greatly aid in constraining and checking our understanding of nuclear effects, such as those associated with shadowing, comover interactions and nuclear absorption. Thus, RHIC measurements will, as a minimum, provide important benchmarks.

We have demonstrated that statistics should be adequate to detect the differences in the Υ'/Υ ratio that would discriminate between different QGP models (assuming that the ratio can be measured at the prompt level). Although this (and other) ratios have the advantage that various systematic effects, as well as the purely nuclear effects associated with shadowing, will cancel, further vital information can be extracted if the p_T spectra for the individual resonances can be measured and the effects of ordinary nuclear shadowing on these spectra unfolded. We have pointed to a comparison with Z production as a potentially useful benchmark in this unfolding process. The ideal situation arises if, in addition to LHC Z data, HERA nuclear data on shadowing is available for the x and Q^2 values appropriate for both onium and Z production at the LHC. The observed p_T spectrum for the Z could be

compared to the prediction based on the Drell-Yan process using the experimentally measured nuclear PDFs from HERA. If there is agreement, then we would have a high level of confidence that we can unfold the shadowing effects on the onia p_T spectra, using the PDFs determined from HERA data at the appropriate x and Q^2 values, so as to expose the impact of the QGP (which hopefully will be dominant over absorption and comovers). Whether or not the HERA data is available, Z production will provide an important benchmark as to how much nuclear shadowing effects alone are likely to be impacting the measured p_T spectra of the onia.

Certain detector features will play a key role in carrying out the analysis as envisioned here. Of greatest importance is the mass resolution in the $\mu^+\mu^-$ channel. The resolution for the CMS detector, as quoted in their technical proposal, is such that the Υ , Υ' and Υ'' resonances can be cleanly separated from one another with very modest background under the peaks. Less certain is the extent to which the $\chi_b \rightarrow \gamma\Upsilon$ process can be separated from direct Υ production by detecting the associated γ for p_T 's in the range of interest. The statistics necessary to discriminate between different QGP models is much greater if the direct 'prompt' Υ'/Υ ratio cannot be isolated. One also would lose the ability to observe the χ_b/Υ ratio, which exhibits sensitivity to the QGP model similar to Υ'/Υ , thus roughly doubling the significance with which different QGP models can be differentiated. It will be important for the LHC detector groups to give further attention to both experimental issues.

Acknowledgements

We would like to thank S. Brodsky, D. Denegri, W. Geist, W. Ko and P. Levai for discussions. We thank U. Baur for providing a Z production program against which to check our results. R.V. thanks the Institute for Nuclear Theory at the University of Washington for its hospitality during the completion of this work.

References

- [1] F. Karsch, Nucl. Phys. **A590** (1995) 367c.
- [2] F.R. Brown *et al.*, Phys. Rev. Lett. **65** (1990) 2491.
- [3] T.K. Gaisser and F. Halzen, Phys. Rev. Lett. **54** (1985) 1754; L. Durand and H. Pi, Phys. Rev. Lett. **58** (1987) 303; G. Pancheri and Y.N. Srivastava, Phys. Lett. **B182** (1986) 199.
- [4] C. Albajar *et al.*, UA1 Collab., Nucl. Phys. **B309** (1988) 405.
- [5] K.J. Eskola and M. Gyulassy, Phys. Rev. **C47** (1993) 2329.
- [6] A.D. Martin, W.J. Stirling and R.G. Roberts, Phys. Lett. **B306** (1993) 145.
- [7] K.J. Eskola, K. Kajantie and P.V. Ruuskanen, Phys. Lett. **B332** (1994) 191.
- [8] K.J. Eskola, Nucl. Phys. **A590** (1995) 383c.
- [9] A.D. Martin, W.J. Stirling and R.G. Roberts, RAL-93-077, J. Phys. **G19** (1993) 1429.
- [10] D.W. Duke and J.F. Owens, Phys. Rev. **D30** (1984) 49.
- [11] A.D. Martin, W.J. Stirling and R.G. Roberts, Phys. Rev. **D50** (1994) 6734.
- [12] H. Satz, Nucl. Phys. **A544** (1992) 371c.
- [13] T. Matsui and H. Satz, Phys. Lett. **B178** (1986) 416.
- [14] F. Karsch, M.T. Mehr, and H. Satz, Z. Phys. **C37** (1988) 617.
- [15] S. Ramos *et al.*, NA38 Collab., Nucl. Phys. **A590** (1995) 117c and references therein.
- [16] M. Gonin *et al.* in proceedings of *Quark Matter '96*, Heidelberg, Germany, P. Braun-Munzinger *et al.*, eds.
- [17] S. Gavin and R. Vogt, Nucl. Phys. **B345** (1990) 104.
- [18] S. Gavin, H. Satz, R.L. Thews, and R. Vogt, Z. Phys. **C61** (1994) 351.
- [19] D. Kharzeev and H. Satz, CERN preprint, CERN-TH-95-214, August 1995.

- [20] S. Gavin and R. Vogt, hep-ph/9606490; S. Gavin and R. Vogt in proceedings of *Quark Matter '96*, Heidelberg, Germany, P. Braun-Munzinger *et al.*, eds.
- [21] CMS Technical Proposal, CERN/LHCC 94-38, LHCC/P1 (1994).
- [22] F. Karsch and H. Satz, Z. Phys. **C51** (1991) 209.
- [23] B. Petersson, Nucl. Phys. **A525** (1991) 237c.
- [24] D.J. Gross, R.D. Pisarski, and L.G. Yaffe, Rev. Mod. Phys. **53** (1981) 43.
- [25] For a recent review, see G.A. Schuler, CERN Preprint CERN-TH.7170/94, February 1994 and references therein.
- [26] M.L. Mangano, P. Nason and G. Ridolfi, Nucl. Phys. **B405** (1993) 507.
- [27] R.V. Gavai *et al.*, Int. J. Mod. Phys. **A10** (1995) 3043.
- [28] G.A. Schuler and R. Vogt, CERN-TH/96-157 and LBL-39012, Phys. Lett. **B** in press.
- [29] CDF Collaboration, Fermilab preprint, Fermilab-Conf-94/136-E, May 1994.
- [30] L. Antoniazzi *et al.*, Phys. Rev. Lett. **70** (1993) 383.
- [31] L. Antoniazzi *et al.*, Phys. Rev. **D46** (1992) 4828.
- [32] B. Ronceux, NA38 Collab., Nucl. Phys. **A566** (1994) 371c.
- [33] K. Ueno *et al.*, Phys. Rev. Lett. **42** (1979) 486.
- [34] T. Yoshida *et al.*, Phys. Rev. **D39** (1989) 3516.
- [35] G. Moreno *et al.*, Phys. Rev. **D43** (1991) 2815.
- [36] F. Abe *et al.*, Fermilab preprint, Fermilab-Pub-95/271-E, August 1995.
- [37] S.J. Brodsky, C. Peterson and N. Sakai, Phys. Rev. **D23** (1981) 2745; S.J. Brodsky, P. Hoyer, C. Peterson and N. Sakai, Phys. Lett. **93B** (1980) 451.
- [38] J. Badier *et al.*, Phys. Lett. **86B** (1979) 98; S. Childress *et al.*, Phys. Rev. Lett. **55** (1985) 1962.

- [39] D. Antreasyan *et al.*, Phys. Rev. Lett. **45** (1980) 863; C. Kourkouvelis *et al.*, Phys. Lett. **91B** (1980) 481; A.L.S. Angelis *et al.*, Phys. Lett. **87B** (1979) 398.
- [40] M. Glück, E. Reya and A. Vogt, Z. Phys. **C53** (1992) 127.
- [41] C. Albajar *et al.*, Phys. Lett. **B186** (1987) 237; K. Eggert and A. Morsch (UA1), private communication in [27].
- [42] N.S. Craigie, Phys. Rep. **47** (1978) 1.
- [43] R. Vogt, Atomic Data and Nuclear Data Tables **50** (1992) 343.
- [44] Particle Data Group, K. Hikasa *et al.*, Phys. Rev. **D45** (1992) S1.
- [45] R. Baier and R. Rückl, Z. Phys. **C19** (1983) 251.
- [46] P. Cho and A.K. Leibovich, Caltech Preprint, CALT-68-1988, May 1995, hep-ph/9505329; Caltech Preprint, CALT-68-2026, November 1995, hep-ph/9511315.
- [47] E. Braaten, M.A. Doncheski, S. Fleming and M.L. Mangano, Phys. Lett. **B333** (1994) 548.
- [48] D.M. Alde *et al.*, Phys. Rev. Lett. **66** (1991) 2285.
- [49] K.J. Eskola, Nucl. Phys. **B400** (1993) 240.
- [50] M.E. Peskin, Nucl. Phys. **B156** (1979) 365.
- [51] G. Bhanot and M.E. Peskin, Nucl. Phys. **B156** (1979) 391.
- [52] D. Kharzeev, H. Satz, A. Syamtomov and G. Zinovjev, CERN preprint CERN-TH/96-72, hep-ph/9605448.
- [53] G. Zinovjev, private communication.
- [54] J. Hüfner and B. Povh, Phys. Rev. Lett. **58** (1987) 1612.
- [55] R. Vogt, S.J. Brodsky and P. Hoyer, Nucl. Phys. **B360** (1991) 97.
- [56] S. Liuti and R. Vogt, Phys. Rev. **C51** (1995) 2244.
- [57] M. Arneodo, Phys. Rep. **240** (1994) 301.
- [58] S. Gavin and M. Gyulassy, Phys. Lett. **B214** (1988) 241.
- [59] J.D. Bjorken, Phys. Rev. **D27** (1983) 140.

- [60] M.-C. Chu and T. Matsui, Phys. Rev. **D37** (1988) 1851.
- [61] J.-P. Blaizot and J.-Y. Ollitrault, Phys. Lett. **199B** (1987) 499.
- [62] F. Karsch and R. Petronizio, Phys. Lett. **212B** (1988) 255.
- [63] J.I. Kapusta, L. McLerran and D.K. Srivastava, Phys. Lett. **B283** (1992) 145.
- [64] R. Vogt, B.V. Jacak, P.L. McGaughey and P.V. Ruuskanen, Phys. Rev. **D49** (1994) 3345.
- [65] X.-M. Xu, D. Kharzeev, H. Satz and X.-N. Wang, Phys. Rev. **C53** (1996) 3051.
- [66] X.-N. Wang and M. Gyulassy, Phys. Rev. **D44** (1991) 3501; Comp. Phys. Commun. **83** (1993) 133.
- [67] J. Collins, D. Soper and G. Sterman, Nucl. Phys. **B250** (1985) 199; J. Collins and D. Soper, Nucl. Phys. **B193** (1981) 381; **B213** (1983) 545(E); **B197** (1982) 446.
- [68] C. Davies, B. Webber and W.J. Stirling, Nucl. Phys. **B256** (1985) 413.
- [69] G. Altarelli, R.K. Ellis, M. Greco and G. Martinelli, Nucl. Phys. **B246** (1984) 12.
- [70] P.B. Arnold and R. Kauffman, Nucl. Phys. **B349** (1991) 381.
- [71] G.A. Ladinsky and C.-P. Yuan, MSUHEP-93/20.
- [72] M.H. Reno, UIOWA-94-01.
- [73] The PHENIX Conceptual Design Report, 1993 (unpublished); PHENIX/Spin Collaboration Report, 1995 (unpublished).
- [74] Z. Lin and M. Gyulassy, Phys. Rev. Lett. **77** (1996) 1222.
- [75] S. Gavin, P.L. McGaughey, P.V. Ruuskanen and R. Vogt, hep-ph/9604369 (1996), Phys. Rev. **C**, in press.
- [76] BRAHMS Conceptual Design Report, 1994 (updated 1995); F. Videbaek, BRAHMS Collaboration, Nucl. Phys. **A566** (1994) 299c.
- [77] J. Ftáčnik, P. Lichard and J. Pišút, Phys. Lett. **B207** (1988) 194.
- [78] S. Gavin, M. Gyulassy and A. Jackson, Phys. Lett. **B207** (1988) 257.

- [79] R. Vogt, M. Prakash, P. Koch and T.H. Hansson, Phys. Lett. **B207** (1988) 263.
- [80] ATLAS Technical Proposal, CERN/LHCC/94-43, LHCC/P2 (1994).
- [81] S.J. Brodsky, A. Hebecker, and E. Quack, hep-ph/9609384.
- [82] B. Kopeliovich and B. Povh, nucl-th/9607035.
- [83] Contributions to ‘Light and Heavy Nuclei in HERA’ subgroup (convenors: M. Arneodo, A. Bialas, M. Krasny, T. Sloan, G. van der Steenhoven, M. Strikman) in Proceedings of *Future Physics at HERA*, eds. G. Ingelman, A. De Roeck, R. Klanner, DESY report.
- [84] These statements are based on the calculations of Ref. [75] for the LHC (using the acceptances of the ALICE experiment).